CAPITAL UNIVERSITY OF SCIENCE AND TECHNOLOGY, ISLAMABAD


# *In Vivo* Toxicity Evaluation of Green Synthesized Silica Nanoparticles from *Euphorbia milii* in Sprague Dawley Rat Model

by

Aneeza Masood

A thesis submitted in partial fulfillment for the degree of Master of Science

in the

Faculty of Health and Life Sciences
Department of Bioinformatics and Biosciences

2024

*I dedicate this thesis to my loving and supportive family and friends who have fully helped me in achieving my life goals.*

# CERTIFICATE OF APPROVAL

**_In Vivo_ Toxicity Evaluation of Green Synthesized Silica Nanoparticles from _Euphorbia milii_ in Sprague Dawley Rat Model**

by

Aneeza Masood

(MBS223018)

## THESIS EXAMINING COMMITTEE

| S. No. | Examiner | Name | Organization |
|---|---|---|---|
| (a) | External Examiner | Dr. Sidra Rehman | COMSATS, Islamabad |
| (b) | Internal Examiner | Dr. M. Asad Anwar | CUST, Islamabad |
| (c) | Supervisor | Dr. Sania Riaz | CUST, Islamabad |

Dr. Sania Riaz
Thesis Supervisor
October, 2024

Dr. Syeda Marriam Bakhtiar
Head
Dept of Bioinfo. and Biosciences
October, 2024

Dr. Sahar Fazal
Dean
Faculty of Health and Life Sciences
October, 2024

# *Author's Declaration*

I, **Aneeza Masood** hereby state that my MS thesis titled "***In Vivo* Toxicity Evaluation of Green Synthesized Silica Nanoparticles from *Euphorbia milii* in Sprague Dawley Rat Model**" is my own work and has not been submitted previously by me for taking any degree from Capital University of Science and Technology, Islamabad or anywhere else in the country/abroad.

At any time if my statement is found to be incorrect even after my graduation, the University has the right to withdraw my MS Degree.


**(Aneeza Masood)**
Registration No: MBS223018

# *Plagiarism Undertaking*

I solemnly declare that research work presented in this thesis titled "***In Vivo* Toxicity Evaluation of Green Synthesized Silica Nanoparticles from *Euphorbia milii* in Sprague Dawley Rat Model**" is solely my research work with no significant contribution from any other person. Small contribution/help wherever taken has been duly acknowledged and that complete thesis has been written by me.

I understand the zero tolerance policy of the HEC and Capital University of Science and Technology towards plagiarism. Therefore, I as an author of the above titled thesis declare that no portion of my thesis has been plagiarized and any material used as reference is properly referred/cited.

I undertake that if I am found guilty of any formal plagiarism in the above titled thesis even after award of MS Degree, the University reserves the right to withdraw/revoke my MS degree and that HEC and the University have the right to publish my name on the HEC/University website on which names of students are placed who submitted plagiarized work.


**(Aneeza Masood)**
Registration No: MBS223018

# *Acknowledgement*

I am profoundly grateful to Allah Almighty for His countless blessings bestowed upon me. I am thankful for everything. His divine guidance and mercy have been my constant companions throughout this journey. I owe a deep depth of gratitude to our University, **Capital University of Science & Technology (CUST)**, for giving me such an opportunity to complete this work. A special thanks to the **Dean & Head** of the Department of Bioinformatics and Biosciences **Dr. Sahar Fazal** & **Dr. Syeda Marriam Bakhtiar** for encouraging and the most of all patience throughout the entire process.

I am especially grateful to my **supervisor, Dr. Sania Riaz,** whose invaluable advice and support were instrumental in the conduction and writing of this thesis. Her guidance, patience, and insightful feedback have been invaluable, and I am fortunate to have had the opportunity to learn from her. I am thankful to the **Department of Pharmacy** for providing animal facilities for my research. Their cooperation and continuous assistance from the staff have greatly facilitated my work and contributed to the successful completion of my experiments.

Special thanks to **Aqsa Zafer**; my thesis would not have been completed without your assistance. Your constant support, encouragement, and willingness to help at every step have been truly remarkable.

Lastly, I am **especially thankful to parents and my sister**, who supported me at every step, making this journey smoother. My family's love, care, and kindness have kept my hope alive, especially during the late nights of hard work. They motivated and uplifted me whenever I needed it. Thank you so much for being ever so selfless. Your belief in me has been a source of immense strength, and your unwavering support has made all the difference.


**(Aneeza Masood)**

# *Abstract*

Silica nanoparticles have gained substantial interest due to their diverse applications. Green synthesis of silica nanoparticles is being studied for their potential in drug delivery, diagnosis, and bioimaging. Before transitioning green-synthesized silica nanoparticles into clinical trials, it is crucial to assess their toxicity through preclinical studies. This study focused on the green synthesis of SiO2 nanoparticle using *Euphorbia milii* leaf extract from sodium metasilicate salt solution to improve biocompatibility and minimize toxicity. Characterization of these nanoparticles was performed using techniques such as FTIR, UV-Vis, XRD, and SEM to confirm their formation. These techniques confirmed the amorphous structure of green synthesized silica nanoparticles by SEM and XRD whose peak range lies within at $\sim$22 $\theta$. The size of nanoparticles generated in this study was 5nm to 20nm. Toxicological assessments were conducted using a Sprague Dawley rat model over 21 days with SiO2 NP doses of 50 mg/kg (low) and 150 mg/kg (high). The study compared control groups, those treated with plant extract, and those receiving nanoparticles. Evaluations included morphological, hematological (WBC, RBC, Hb, MCV, MCH, MCHC, platelet count), liver function (ALT, AST, ALP, albumin, total bilirubin), renal parameters (BUN, creatinine), and inflammatory markers (CRP, ESR). While the low-dose group showed minimal changes from controls, the high-dose group exhibited notable histopathological effects, such as altered cellular morphology and liver fatty infiltration. These findings suggest that green-synthesized $SiO_2$ NPs are less toxic and more biocompatible than chemically synthesized alternatives, highlighting their potential for safer biomedical use. The primary aim of the study was to biosynthesize silica nanoparticles from *Euphorbia milii* extract and evaluate their safety profile, providing insights for their future biomedical applications.

# Contents

# List of Figures

# List of Tables

# Abbreviations

| | |
|---|---|
| **ALP** | Alkaline phosphatase |
| **ALT** | Alanine transaminase |
| **AST** | Aspartate Aminotransferase |
| **AgNPs** | Silver nanoparticles |
| **AuNPs** | Gold nanoparticles |
| **CRP** | C-reactive proteins |
| **DSS** | Drug delivery system |
| **EDTA** | Ethylenediaminetetraacetic acid |
| **EDX** | Energy dispersive X-ray |
| **ESR** | Erythrocyte Sedimentation Rate |
| **FTIR** | Fourier-transform infrared spectroscopy |
| **Hb** | Hemoglobin |
| **LFT** | Liver function test |
| **MCH** | Mean corpuscular hemoglobin |
| **MCHC** | Mean corpuscular hemoglobin concentration |
| **MCV** | Mean corpuscular volume |
| **NMs** | Nanomedicines |
| **NP** | Nanoparticles |
| **RBC** | Red blood cells |
| **RFT** | Renal function test |
| **ROS** | Reactive oxygen Species |
| **SEM** | Scanning electron microscopy |
| **$SiO_2$** | Silica dioxide |
| **TEOS** | Tetraethyl Ortho-silicate |

**WBC** White blood cells

**XRD** X-ray diffraction

# Chapter 1

# Introduction

Nanotechnology has emerged as a revolutionary field with vast applications across various scientific and industrial sectors. Nanoparticles are key components of nanotechnology as their size range from 1 to 100nm, that's responsible for its unique physical and chemical properties [1]. In biology, nanoparticles have garnered significant interest for their potential applications in drug delivery, imaging, biosensing, and therapeutic treatments due to their ability to interact at the molecular and cellular levels [2].

Silica nanoparticles ($SiO_2$ NPs) are seeking more attention in medicine for their biocompatibility, stability, and versatile surface chemistry. They are used in biomedical applications such as imaging contrast agents, biosensors, gene delivery vehicles, and scaffolds for tissue engineering [3].

Silica nanoparticles can be synthesized using various methods, including chemical, physical, and biological approaches. Chemical methods involve the use of harmful and toxic chemicals, which may pose environmental and health risks. Physical methods often require high energy input and specialized equipment, and Physical methods have drawbacks like space requirements, and lengthy thermal stabilization, particularly with traditional tube. In contrast, green synthesis utilizes natural sources such as plant extracts, reducing agents, and stabilizers to produce nanoparticles in a sustainable and eco-friendly manner. This approach

not only minimizes environmental impact but also enhances the biocompatibility of nanoparticles [4].

Green synthesis using plant extract offers several advantages over traditional methods [2]. Plants contain bioactive compounds that are used as source of stabilizing and reducing agents, facilitating process of formation of silica nanoparticles. Euphorbia milli, commonly known for its medicinal properties, has shown promising source for synthesis of silica nanoparticles due to its phytochemical composition and property to reduce silica precursors effectively. The controlled synthesis of silica nanoparticles ensures their suitability for specific medical applications while minimizing potential toxicity concerns.

*Euphorbia milii* , known as crown of thorns, has been traditionally used in various medicinal practices for its anti-inflammatory, antimicrobial, and wound-healing properties. Extracts from this plant are rich in bioactive compounds that contribute to its therapeutic potential, making it an important way for green synthesis of silica nanoparticles with enhanced biological activities [5].

The characterization of green synthesized silica nanoparticles involves detailed analysis of their physical, chemical, and structural properties. Techniques such as Scanning Electron Microscopy (SEM), X-ray Diffraction (XRD), and Fourie r Transform Infrared Spectroscopy (FTIR) are utilized to examine particle size, crystallinity, and surface functional groups. These insights are important for optimizing synthesis protocols and understanding nanoparticle behavior in biologicalenvironments [6].

$SiO_2$ NPs are valued in nanotechnology for their biocompatibility, and low toxicity, essential for biomedical tools like biosensors and drug delivery systems, so $SiO_2$ NPs safety is to be ensured. Larger silicon materials are generally safe, nanoparticles like silver and gold have shown varying levels of toxicity. Studies on $SiO_2$ NPs have produced conflicting results: some suggest inflammatory responses and cell damage, while others indicate minimal harm. This highlights the need for thorough evaluation to ensure safe and beneficial use of $SiO_2$ NPs in medical and technological applications [7].

The aim of the study was to green synthesize $SiO_2$ NPs using plant extract that can help to stabilize and reduce $SiO_2$ NPs at room temperature without using any toxic or hazardous materials. Assessing the safety of silica nanoparticles synthesized from *Euphorbia milii* is critical before their clinical translation. Toxicity studies in albino Sprague Dawley (SD) rats involve administering varying doses of nanoparticles and monitoring physiological parameters, histopathological changes in vital organs, and biochemical markers in blood and serum that helped to identify any adverse effects and establish safe dosage ranges for future biomedical applications.

## 1.1 Hypothesis

The green synthesized silica nanoparticles using *Euphorbia milii* and administering their low and high doses to Sprague Daw rats may have biochemical, hematological and histopathological minimal toxicity.

## 1.2 Problem Statement

The lack of comprehensive studies on the toxicity of silica nanoparticles synthesized using *Euphorbia milii* extract through green synthesis methods represents a significant gap in current scientific literature. This gap impedes the exploration of environmentally sustainable approaches to evaluate the safety of plant-derived nanoparticles.

## 1.3 Aim and Objectives

The aim of this research was to investigate the potential of *Euphorbia milii* plant extract to synthesize the silica nanoparticle from sodium metasilicate via green synthesis and to assess their toxicity at different levels. To achieve this aim following objectives are aligned accordingly:

1. Eco-friendly green synthesis of silica nanoparticles (NPs) using the extract of *Euphorbia milii*.

2. To characterize the green-synthesized silica nanoparticle by different methods.

3. To evaluate the low and high dose toxicity and safety profile of silica nanoparticles using rat model

# Chapter 2

# Literature Review

## 2.1 Nanoparticles

Nanotechnology has emerged as a revolutionary field with vast applications across various scientific and industrial sectors. Nanoparticles are key components of nanotechnology as their size range from 1 to 100nm, that's responsible for its unique physical and chemical properties [8].

The "nano" prefix comes from Greek language for very small and refers to one-billionth (10∧-9), and "nanotechnology" was first used by Norio Taniguchi. This field focuses on manipulating materials at the nanoscale to harness their unique properties. As an interdisciplinary science, nanotechnology holds great promise for transforming various scientific and industrial fields. Its applications span a wide range, including biomolecular detection and diagnostics, therapeutic solutions, catalysis, microelectronics, DNA sequencing, optical technologies, pharmaceuticals, and sensor development [2].

### 2.1.1 Physicochemical Properties

Nanoparticles represent unique physicochemical properties that are suitable for a many application. Some of the most important properties include electronic, optical, magnetic, mechanical, and thermal characteristics.

#### 2.1.1.1 Optical Property

The optical properties of noble metal nanoparticles depend heavily on their size, showing a clear visible extinction band on ultraviolet spectrum that doesn't appear in bulk metals. This band forms when the frequency of incoming light matches the collective movement of electrons, known as Localized Surface Plasmon Resonance (LSPR). The LSPR peak wavelength changes based on the nanoparticles' size, shape, and spacing between them [9].

#### 2.1.1.2 Mechanical Property

Nanoparticles possess distinctive mechanical characteristics, including flexibility, resilience, and strength under tension, that are significant for their use in areas such as friction management, surface treatment, nanoscale production, and nanomanufacturing.

Key factors include stiffness, hardness, stress and strain, adhesion, and friction. These properties are also influenced by surface coatings, clumping, and lubrication. The difference in rigidity between nanoparticles and the surfaces they interact with determines whether they will be dented or deformed under pressure, which is essential for improving surface quality and material removal [10].

#### 2.1.1.3 Magnetic Property

Magnetic nanoparticles are highly valued in fields like catalysis, biomedicine, data storage, , and environmental cleanup. They work best when their size is below a critical range of <10–20 nm, allowing their magnetic properties to be most effective. At such a small scale the magnetic properties of NPs become quite prominent. This makes them valuable and useful for many diverse applications. These properties arise from uneven electron distribution, which is affected by the synthesis process. Terms such as conductivity, semi-conductivity, and resistivity describe their magnetic and electrical characteristics, making them ideal for contemporary electronic applications [11].

#### 2.1.1.4 Thermal Property

Transfer of heat in nanoparticles relies on electron transmission/conduction, lattice vibration, and scattering phenomena. Nanoparticles thermal properties, including conductivity, power of thermoelectricity, holding capacity of heat, and stability, are significant.

For example, thermal conductivity of copper is 700 times higher than water at room temperature. Furthermore, this is 3000 times higher than engine oil. Water thermal conductivity is also lower than oxides like alumina (Al2O3). Size of NP directly depends on thermal conductivity of nanoparticles and electrical conductivity, with smaller NPs having higher surface-to-volume ratios, facilitating better heat transfer [12].

#### 2.1.1.5 Catalyst

Nano-catalysis employs NP as catalysts, offering improved catalytic properties compared to bulk materials. NP catalytic effectiveness depends on size, form, state, composition, spacing between the particles, state of oxidation, and material support.

Smaller NPs are more catalytically active due to quantum effects and increased surface-to-volume ratios, while different shapes influence reactivity. Alloying NPs enhances activity by changing electronic properties and reducing poisoning effects. Interparticle spacing affects stability, with closer spacing leading to faster deactivation [13].

### 2.1.2 Classification of Nanoparticles

#### 2.1.2.1 Based on Materials Classification of Nanoparticles

Nanoparticles can be categorized into organic, inorganic and carbon nanoparticles.

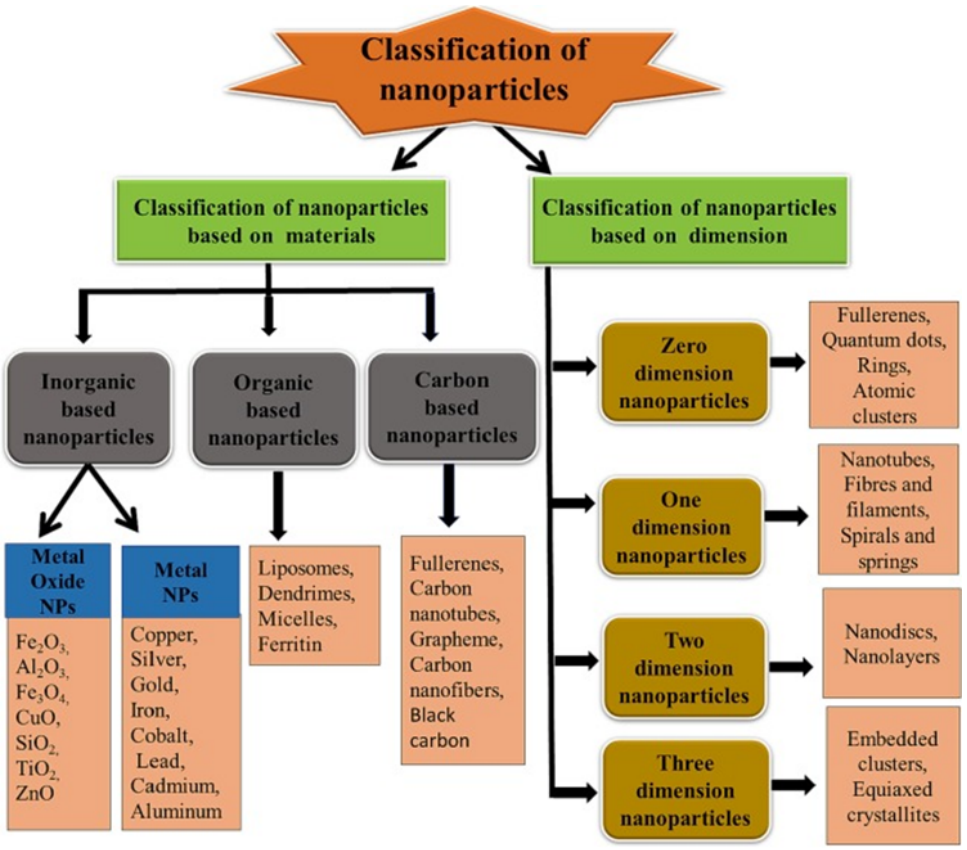


FIGURE 2.1: Material and dimension-based classification nanoparticles [3]

- Inorganic nanoparticles, these nanoparticles do not contain carbon molecules in their structure consists of metals and nonmetallic compounds. Metal nanoparticles, This category features metals like Silver (Ag), Gold (Au) and Aluminum (Al). They are distinguished by their unique properties related to their size, surface area, pore size, surface charge density, shape that can be spherical and cylindrical, color, and crystalline form. Metal-Oxide nanoparticles, these metal nanoparticles react with oxygen to form oxides, enhancing their properties and reactivity. Examples include Titanium-Oxide (TiO2), Silicon-Oxide (SiO2), Iron-Oxide (Fe2O3) and Zinc-Oxide (ZnO) [14].

- Organic nanoparticles, known as nano-capsules, this group consists of liposomes like materials. They are characterized by their unique size, form, composition, and surface-morphology [14].

- Carbon-Based nanoparticles are composed containing carbon materials, like graphene, fullerenes, carbon nanofibers, carbon nanotubes, and black carbon.

#### 2.1.2.2 Dimension Based Classification

Nanoparticles can also be classified based on their dimensions as zero dimensional-0D nanoparticles, the most common type of nanomaterials, that have rings, spheres atomic clusters, fullerenes, and quantum dots. One dimensional-1D nanoparticles, these include nanofibers, nanotubes, nano-spirals, and nano-rods, which have single dimension that exceeds nanoscale. Two dimensional-2D This class includes nano-layers, nano-discs, nano-films, and nano-coatings, characterized by two dimensions at the nanoscale.

Three dimensional-3D nanoparticles, despite their components being less than 100 nm, all three-dimensions of these nanoparticles exceed 100 nm. They are formed by combining nanoscale particles [14].

TABLE 2.1: Represent general classification of nanoparticles

| **Class** | **Description** | **Examples** | **Morphology** | **Ref** |
|---|---|---|---|---|
| **Metallic Nanoparticles** | Composed of metallic elements or alloys | Gold (AuNPs), Silver (AgNPs), Iron (FeNPs) | Spherical shaped | [15] |
| **Metal Oxide Nanoparticles** | Composed of metal oxides | Titanium dioxide (TiO2NPs), Zinc Oxide (ZnONPs), Silica (SiO2NPs) | Spherical, Nanorods, Nanosheets, Nanowires | [16] |
| **Carbon-based Nanoparticles** | Composed of carbon-based materials | Carbon nanotubes (CNTs), Fullerenes (C60), Graphene oxide (GO) | Nanotubes, Nanospheres, Graphene sheets | [17] |
| **Lipid-based Nanoparticles** | Composed of lipids or lipid-like materials | Liposomes | Spherical, Multilamellar, Unilamellar | [18]. |

**Table 2.1 continued from previous page**

| Class | Description | Examples | Morphology | Ref |
|---|---|---|---|---|
| | | Solid lipid nanoparticles (SLNs), Nanoemulsions<br>Carriers of lipid | | |
| **Polymer Nanoparticles** | Composed of polymers or polymer composites | Poly (lactic-coglycolic acid) (PLGA) nanoparticles | Spherical, Nanofibers, Dendritic | [19] |
| **Hybrid Nanoparticles** | Composed of a combination of materials | Silica-coated gold nanoparticles,<br>Polymer-coated magnetic nanoparticles | Core-shell, Janus, | [20] |

## 2.2 Nanomedicine

Nanomedicine has revolutionized pharmaceutical development, recognized in the European Union as a pivotal technology. It utilizes nanoparticles with specific physicochemical properties for enhanced drug delivery, pivotal in drug research and development.

Nanomaterials serve three main medical purposes: controlling drug delivery (nano therapy), disease diagnosis (nano diagnosis), and regenerative medicine, leveraging their intrinsic properties [21].

While nano therapy and nano diagnosis have been traditional methods, nowadays regenerative technology is trendy. focuses on using nanotechnology to manipulate genetically modified stem cells for curing genetic disorders.

Biodegradable nanoparticles like carbon nanofibers and collagen nanofibers play a critical role in tissue engineering and implantable materials, particularly in treating disorders like Alzheimer's and Parkinson's diseases [22].

Nanotechnology has significantly advanced precision gene therapy by delivering medicine directly to DNA, targeting diseases rooted in genetic mutations. This approach has enabled the development of therapies for cancers, Alzheimer's, Parkinson's, and other genetic disorders, enhancing pharmaceutical research and clinical applications [23].

Effective gene therapy relies on precise drug delivery mechanisms that avoid healthy cells and target specific diseased cells. Nanoparticles are engineered to exploit tumor characteristics, such as enhanced vascularity and permeability, through passive and active targeting methods. Passive targeting utilizes the Enhanced Permeability and Retention (EPR) effect, while active targeting employs specific ligands to bind receptors overexpressed on target cells, ensuring effective drug delivery [23] [24].

Tumor targeting is divided into passive and active methods. Passive targeting takes advantage of the distinct features of tumors, such as their enhanced vascularity and permeability, and relies on the size and circulation time of nanoparticles (NPs). The Enhanced Permeability and Retention (EPR) effect, vital for passive targeting, is influenced by factors like angiogenesis, perivascular tumor invasion, and intratumor pressure, along with NP characteristics (Fig 2.2).

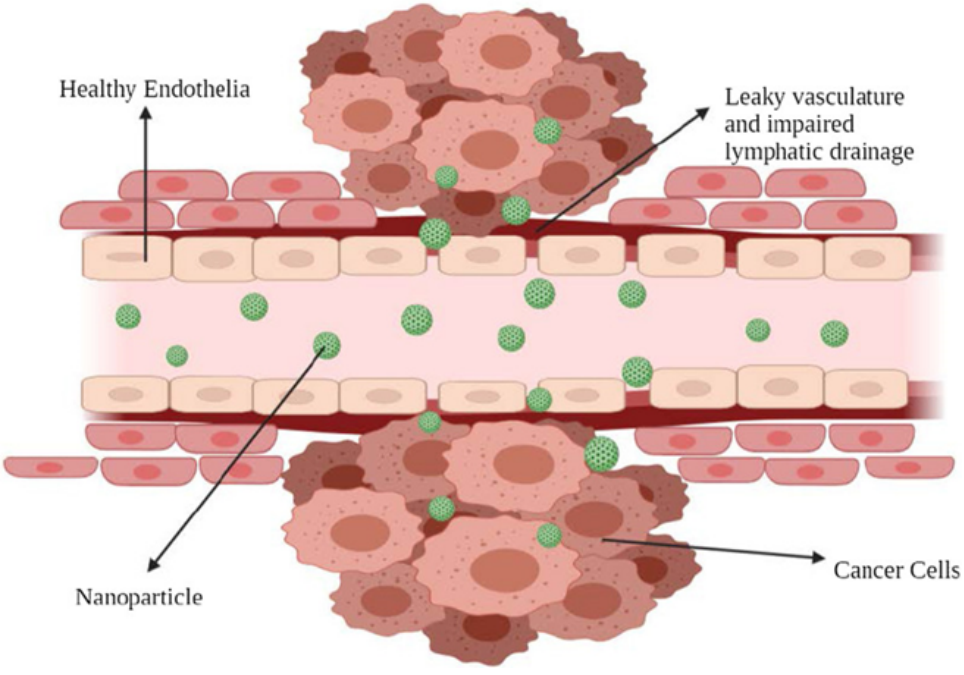


FIGURE 2.2: Passive Targeting [23].

Active targeting employs specific ligands (e.g., transferrin, folate) that bind to overexpressed receptors on target cells, enhancing nanoparticle (NP) affinity and retention for improved drug delivery (Fig 2.3).

Key receptors involved include transferrin, folate, and epidermal growth factor (EGFR) receptors. Examples include transferrin-modified NPs for ovarian carcinoma and strategies to disrupt tumor blood supply, inducing hypoxia and necrosis. pH-sensitive drug delivery systems leverage the acidic tumor environment to enhance treatment efficacy.

An ideal nanocarrier combines high cargo capacity, biocompatibility, stability, uniformity in size and shape, and targeted release capabilities. Porous inorganic materials like Mesoporous Silica Nanoparticles (MSNs) and Metal-Organic Frameworks (MOFs) forms of silica NPs, are particularly promising due to their adjustable chemistry and stability.

Silica NPs can encapsulate drugs and precisely release them in response to pH changes, reactive oxygen species, temperature, enzymes, or light. Researchers have developed dual-responsive peptides like for MSNs, exploiting the acidic tumor environment to enhance drug delivery effectiveness [23].

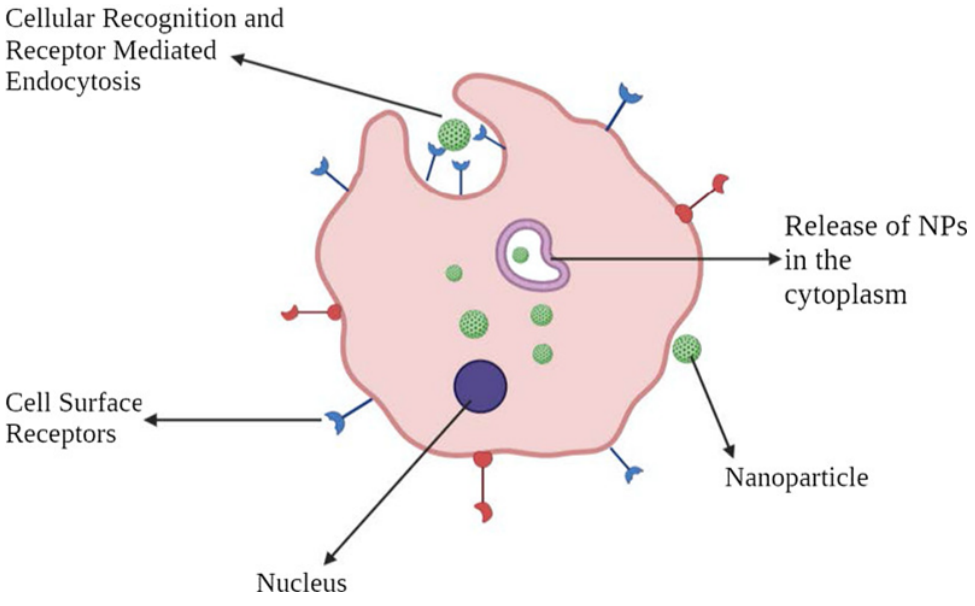


FIGURE 2.3: Active Targeting [23]

## 2.3 Synthesis Approach for Nanoparticles

Nanoparticles come in various shapes, sizes, and structures, achieved through different synthesis methods. These methods are broadly used and have two categories: top-down and bottom-up approaches (Fig 2.4), each with condition of reactions and operations-based subclasses.

### 2.3.1 Top-Down Approach

Constructive method has assembling materials that are atoms or molecules to make clusters and eventually nanoparticles. Common techniques include spinning, sol-gel formation, chemical vapor-deposition (CVD), laser-pyrolysis, biosynthesis and plasma spraying synthesis [25].

### 2.3.2 Bottom-Up Approach

It is well-known for its process, which breaks down huge materials into smaller pieces that become NPs. Among the methods are thermal breakdown, chemical etching, laser ablation, mechanical milling, and nano-lithography. By changing the synthesis parameters and reaction circumstances, one can modify the size, shape, and charge of nanoparticles [26].

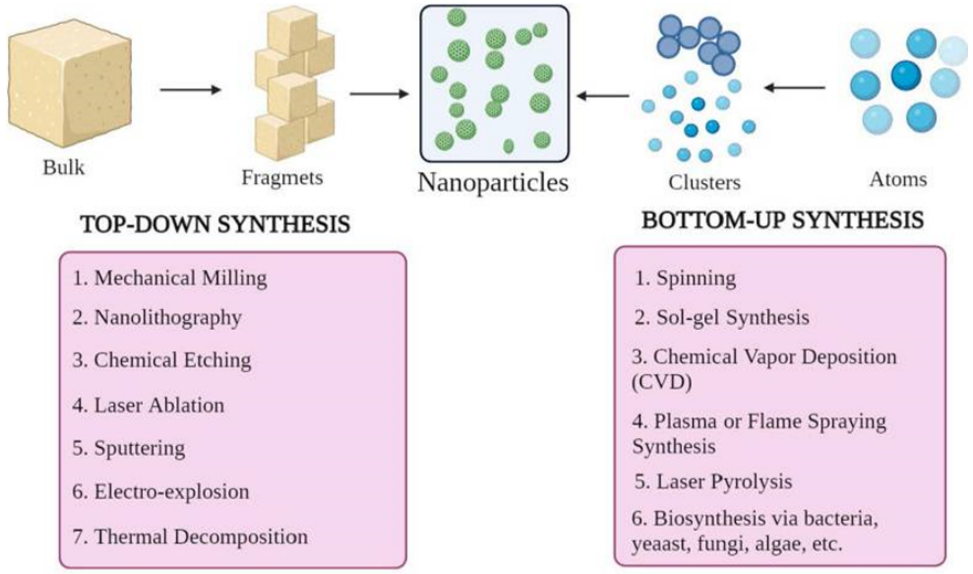


FIGURE 2.4: Top-down and Bottom-up approach classifications [23]

## 2.4 Nanoparticles Synthesis

### 2.4.1 Physical Synthesis

Several physical methods are utilized to produce nanoparticles, each with distinct benefits and applications. The plasma method uses Radio Frequency (RF) heating coils to create plasma, where metal vapor nucleates on helium gas atoms and is then collected as nanoparticles. CVD involves the chemical reaction of volatile precursors on a heated substrate, resulting in the formation of ultrafine particles and thin films.

Microwave irradiation accelerates chemical reactions, improving yields and reducing reaction times for the synthesis of organic, inorganic, and hybrid materials. The pulsed laser method produces nanoparticles by generating hot spots on a rotating disc exposed to laser pulses, commonly employed to produce silver nanoparticles. Finally, gamma radiation offers a reproducible, straightforward, and cost-effective method for synthesizing metallic nanoparticles, using minimal reagents and producing monodisperse particles with controlled shapes. These techniques showcase the versatility and potential of physical methods in nanoparticle synthesis [27].

### 2.4.2 Chemical Synthesis

The polyol method, microemulsions, thermal decomposition, and electrochemical synthesis are chemical approaches for synthesizing nanoparticles, each offering unique advantages and applications. The polyol method utilizes nonaqueous solvents like ethylene glycol, serving as both solvent and reducing agent, to control nanoparticle size and morphology, ideal for large-scale production. Microemulsions, involving liquid-in-liquid dispersions stabilized by surfactants, enable the synthesis of inorganic nanoparticles with controlled size and shape through Brownian motion-induced nucleation. Thermal decomposition involves heat-induced chemical breakdown of compounds, providing insights into decomposition mechanisms and products. Electrochemical synthesis, conducted in electrochemical cells,

allows precise control over reaction conditions to produce nanoparticles, such as silver and platinum, with varied sizes and high purity [27].

## 2.5 Green Synthesis

Traditional methods have been widely used, but recent studies highlight green synthesis as the most effective approach for creating NPs, offering lower failure rates, cost savings, and easier characterization. Unlike physical and chemical methods, green synthesis produces distinct particles by utilizing biological components like plant extracts instead of expensive chemical agents. This bottom-up method parallels chemical approaches but is more environmentally friendly, sustainable, and scalable. Green synthesis also allows for the recycling of valuable metal salts from waste streams, making green synthesis prepared NPs preferable for their superior qualities compared to conventionally synthesized NPs. The use of hazardous chemicals in traditional methods can enhance particle reactivity and toxicity, posing risks to health and the environment, whereas green synthesis methods are chosen for their reduced nanoparticle toxicity, leading to a growing adoption of plant extracts in NP synthesis [4].

The concept of green synthesis has emerged as a sustainable alternative for nanoparticle fabrication. This approach harnesses natural resources, such as plant extracts, to synthesize nanoparticles, utilizing them as both stabilizing and reducing agents. Plant extracts are rich sources of bioactive compounds like polyphenols, flavonoids, and terpenoids, which play a crucial role in reducing metal ions and ensuring the stability of the resulting nanoparticles. Furthermore, green synthesis offers numerous benefits, including cost-effectiveness, scalability, and minimized environmental impact [32]. Complex metallic ions can be reduced by Plants to generate simple ions that become the source of medicinal compounds [28].

Recently, several in vivo techniques have emerged, utilizing herbal extracts as reducing agents to synthesize nano-sized materials [29]. A variety of plant species, along with different acids and metal salts (such as Au and Ag), have been utilized in the green synthesis of nano-sized materials [30]. Compared to methods involving

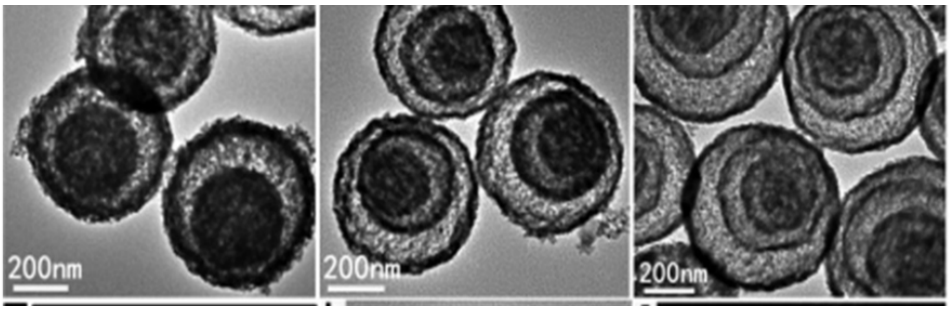


FIGURE 2.5: TEM of the CO3O4 hollow microspheres [31]

microorganism and chemicals that are harmful, the utilization of plant materials for nanoparticle fabrication is more advantageous due to the absence of bacteria or toxic chemical contaminants. Moreover, this requires low energy and offers simplicity, as well as versatility in applications [31]. In the eco-friendly synthesis of nanoparticles, a wide range of plant extracts obtained from different plants parts like flowers leaves, stems, roots, seeds, and fruit, have been employed.

## 2.6 Characterization

### 2.6.1 Morphology Characterization

The morphological characteristics of NPs are crucial as they significantly impact their properties. Various techniques are used for morphological analysis, with microscopic methods like Transmission Electron Microscope (TEM) Polarized Optical Microscopy (POM), Scanning Electron Microscopy (SEM) [33].

SEM is a widely used technique for examining nanoparticle morphology and dispersion within bulk materials or matrices. For instance, SEM has revealed the distribution of Single-Walled Carbon Nanotubes (SWNTs) in Poly(butylene) Terephthalate (PBT) and nylon-6 [30]. POM has shown star-like spherulites, which decrease in size with more SWNTs. TEM works on electron transmittance principles, offering detailed information from low to high magnification. TEM has identified the quadrupolar hollow shell structure of Co3O4 nanoparticles (Fig 2.5), advantageous for Li-ion battery anodes due to their enhanced cycling performance and specific capacity [34].

### 2.6.2 Structural Characterization

Structural characteristics are crucial for analyzing the components tha compose and bind in nature of materials, offering insights into their bulk properties. Common techniques such as X-ray Diffraction (XRD), Energy Dispersive X-ray (EDX), Raman spectroscopy and Zeta size analysis are employed to identify the properties of structures of nanoparticles.

The XRD technique is most commonly used and particularly suitable for powdered samples obtained directly from drying their respective colloidal solutions. Using XRD equipment, the positions and peak intensities of sample's diffraction pattern are compared with reference patterns from various databases. This comparison aids in determining the composition of nanoparticles quantitatively [35].

The XRD method operates by directing X-rays at nanoparticles, causing them to scatter due to the movement of electrons around the atoms' nuclei. These scattered X-rays create interference patterns, where constructive interference occurs when waves are in phase and destructive interference when they are out of phase. The arrangement of atoms at the atomic scale directly influences the diffraction pattern: shorter periodic arrangements of atoms lead to higher diffraction angles, and vice versa [36].

### 2.6.3 Optical Characterization

For optical property characterization of the nanoparticle Ultraviolet–Visible (UV-Vis) spectroscopy is used, it is a technique that helps to measure the light that is visible given sample absorption or transmittance compared to the sample or blank sample of their reference. As this technique depends on properties of light, light contains the energy that is inversely proportional to the wavelength, meaning that particle that have short wavelength have more capability to carry the energy and vice versa. So, the value of the absorbance is basically the energy that is required by the electron to promote in a substance to a high energy level. This is the reason that there is different absorbance of light at the different wave lengths. The visible light range is from 380nm that is violet to 780nm that is of red spectrum. The

UV-Vis spectroscopy helps to determine the particles by pointing their wavelength at which they absorb maximum light energy [37].

## 2.7 Nanotoxicology

Given the ubiquitous application of nanoparticles, awareness of their effects on human well-being and the natural environment is imperative. Although nanoparticles have many advantages, misuse and improper handling can lead to toxicity and environmental damage. Numerous in-vitro and in-vivo research conducted in the field of nanotoxicology—the study of nanoparticle toxicity—have demonstrated that the size and surface area of nanoparticles make them extremely reactive, which raises the possibility of toxicity. The production of Reactive Oxidative Species (ROS)s, which harm biological macromolecules, is frequently the cause of this toxicity [38].

### 2.7.1 Nanotoxicity Induced by ROS Generation

One of the main mechanisms underlying nanotoxicity is the production of ROS, which can result in DNA damage, aberrant cell signaling, alterations in cell motility, cell death, apoptotic and cancer. The chemical makeup of designed nanomaterials determines how much ROS is produced by them. These nanomaterials are more cytotoxic and genotoxic than their bulk equivalents because of their small size, substantial specific surface area, and severe surface reactivity. They also create higher quantities of ROS. Numerous nanomaterials have been discovered to cause ROS-mediated toxicity in biological systems, such as skin fibroblasts and human erythrocytes. According to research, the generation of ROS is how quantum dots, silica nanoparticles, and nano-CuO cause oxidative stress and cytotoxicity. ROS are also produced by nano-ZnO and nano-TiO2, which can cause oxidative damage, inflammation, and cell death [39].

Both nano-Au and gold–cobalt nanoalloys have been explored for biomedical applications. As in study [40], found that in mice, the gold–cobalt nanoalloy altered

tumor-initiating genes, increased micronuclei formation, and generated 8-OHdG, while nano-Au exhibited much lower toxic activities. These toxic effects are attributed to increased oxidative stress [41].

### 2.7.2 Nanomedicine and Toxicity

Only in the past two decades has the word nanotoxicology attracted more attention. Since then, significant progress has been made in this field [42]. Since they can both study the same mechanisms and have an impact on the same metabolic pathways, nanomedicine and nanotoxicology are inextricably intertwined [43]. At the intersection of toxicology and nanomedicines, nanotoxicology has developed into a subdiscipline. Nanomaterials (NMs) have different properties from their bigger equivalents due to their extremely small size and high surface area to volume ratio, which may lead to unanticipated interactions with cells and tissues. The potential hazardous interactions between NMs and various biological systems (cells, tissues, and living beings) are frequently highlighted by nanotoxicology [42].

Over several years of research, it has been clear that the interactions between nanomedicines and living things' cells are quite intricate. The potential impact of NMs' morphological and physicochemical features on these interactions is unknown, though [44].

The physical and chemical properties of nanomedicines have a significant influence on how they interact with biological cells and can also have an impact on their toxicity. Nanotoxicology is responsible for examining the harmful effects of nanomedicines because the size of the materials has a significant influence on their toxicity. Numerous elements, such as size, area of surface, form, content, surface chemistry, aggregation/agglomeration procedures, etc., constitute the basis of nanotoxicology [45].

### 2.7.3 Toxicity of Gold Nanoparticles

Gold nanoparticles (AuNPs) have been the subject of extensive research due to their distinctive physical, chemical, and optical properties and are now used in many different sectors. However, depending on criteria including size, shape, surface chemistry, concentration, and length of exposure, gold nanoparticles, like any other nanomaterial, can exhibit varying degrees of toxicity [46].

The toxicity of AuNPs is significantly influenced by their size and structure. Smaller nanoparticles have a greater ability to infiltrate cells and tissues, which could increase their toxicity.

Additionally, the toxicity of substances can vary depending on how they interact with biological systems. Cells can absorb AuNPs using several different processes, including endocytosis. Their buildup inside of cells can impair biological processes and have harmful effects [47].

ROS can be produced within cells because of oxidative stress brought on by AuNPs. Excessive ROS can harm DNA, lipids, proteins, and other biological components, which may ultimately cause cell death. Inflammation and immunological responses can be brought on by AuNPs [42].

This might contribute to tissue injury by causing the release of pro-inflammatory cytokines and the activation of immune cells. The genotoxic properties of gold nanoparticles raise the possibility that they could contaminate DNA and cause genetic alterations [48].

The organ or tissue being researched can affect how harmful AuNPs are. For instance, compared to the lungs or brain, the liver may respond to nanoparticles differently. The toxicity of nanoparticles depends on their capacity to be eliminated by the body. Long-term harm could result from nanoparticle accumulation and ineffective removal [46].

### 2.7.4 Toxicity of Silver Nanoparticles

Silver Nanoparticles (AgNPs) have also attracted a lot of attention due to their unique properties and potential applications in a range of industries, including consumer products, health, and electronics. However, just like other nanoparticles, AgNPs can demonstrate toxicity based on their characteristics and the conditions of their exposure [49].

According to certain research, these nanoparticles may be mutagenic and cause DNA damage, among other genotoxic effects. AgNPs are extensively distributed throughout the body and, with a single encounter, alter gene expression [50].

By producing reactive oxygen species, AgNPs can cause oxidative stress by ROS. ROS can harm tissues and cells, resulting in cell death, DNA damage, and inflammation [51]. Body weight and locomotor activity were both reduced by AgNPs [52].

Similar to gold nanoparticles, silver nanoparticles can trigger an immune response and inflammation. This immune activation can contribute to tissue damage and other adverse effects. AgNPs have the greatest impact on the immune system, which results in decreased thymus weight [53].

AgNPs toxicity is primarily caused by their intact nanostructure, with just a little amount coming from the released silver ions. AgNPs may accumulate largely in the liver and spleen in addition to other tissues [54][55].

### 2.7.5 Toxicity of Silica

Since chemically manufactured silica nanoparticles can be easily modified as drug carriers, they are valuable in drug delivery. They comprise roughly 8% of airborne nanoparticles and are also present in the atmosphere. Despite being thought to be quite safe for use in medicine, silica nanoparticles have been linked to oxidative stress due to their ability to produce ROS.

Human lung cells treated to silica NPs (15-46 nm) at dosages ranging from 10 to 100 $\mu$g/mL showed elevated levels of ROS, lactate dehydrogenase (LDH), and malondialdehyde. Liver cells exposed to silica-based NPs (70 nm) at 30 mg/kg exhibited biochemical alterations and symptoms of liver injury. These findings demonstrate that, while silica nanoparticles are adaptable for medicinal applications, their possible health consequences must be carefully examined [56].

### 2.7.6 Toxicity Mitigation

Nanoparticles are valuable in medicine but pose toxicity challenges. To address this, strategies focus on modifying NP surfaces. Coating NPs with materials like Polyethylene Glycol (PEG), Polyvinylpyrrolidone (PVP), and zwitterionic polymers alters their properties, reducing toxicity.

PEGylation improves biocompatibility and stability. Adjusting NP surface chemistry, such as charge and hydrophobicity, also lowers toxicity and enhances effectiveness (Fig 2.6). Another approach involves coating NPs with natural cell membranes e.g., from Red Blood Cells (RBCs) or White Blood Cells (WBCs), which enhances safety and targeting abilities. These efforts aim to make metal-based NPs safer and more effective for biomedical uses [57].

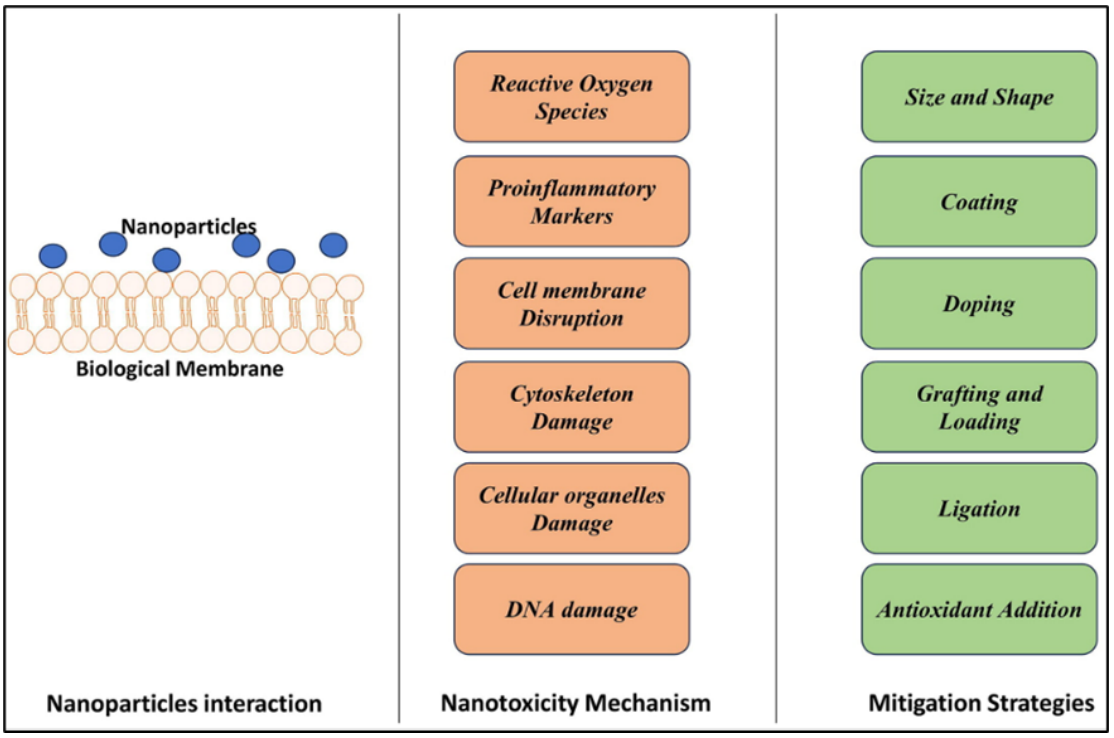


FIGURE 2.6: Ways that can mitigate nanoparticles toxicity strategies [57]

## 2.8 Drug Delivery System

Drug delivery is the process of providing pharmacological chemicals to accomplish therapeutic effects. It comprises a variety of tactics for increasing therapeutic efficacy, improving patient compliance, and reducing adverse effects.

Traditional methods like oral ingestion and injections are supplemented by advanced technologies such as nanotechnology and carrier systems. These innovations optimize drug distribution, release kinetics, and site-specific targeting, aiming to deliver medications precisely where needed in the body [58].

### 2.8.1 Conventional Nanoparticle Drug Delivery

Nanoparticles can enter the human body through direct injection, inhalation, and oral intake. Then start to circulation inside the body, protein interaction occurs because of that distribute in various organs. Distributing and eliminating the nanoparticles is done by lymphatic system, filtering excess fluid and detecting

foreign matter. The affect their distribution, toxicity, and targeting ability of the nanoparticles depends on its shape and size and affect the toxicity and distribution. Smaller particles have a larger surface area, leading to faster drug release, but they should be made in such a way that they clearance by the lymphatic system [59].

### 2.8.2 Targeted Nanoparticle Drug Delivery

Targeted delivery of drug involves creating nanoparticles that can reach, recognize, bind, and deliver drugs to specific pathological tissues reducing damage to tissues that are healthy. This can be done by active targeting system, where drug carriers are conjugated to tissue-specific ligands, or passive targeting, where nanoparticles reach target organs due to leaky junctions in inflamed or damaged tissue. Targeting ligands might be tiny compounds, peptides in antibodies, proteins, or nucleic acid aptamers. Liposomes, which resemble cell membranes, may be adjusted in size and charge by using particular lipid monomers, as well as surface targeting ligands, to improve lipophilic drug delivery to specified cells. This smart multifunctional drug-loaded nanoparticle system represents a significant advancement in targeted drug delivery [59].

### 2.8.3 Drug Delivery System (DSS) to Treat Diseases

Lipid-Based drug delivery system like liposomes and micelles. Liposomes are hydrophobic and hydrophilic drug delivery vehicles that resemble bilayer nanovesicles seen in cell membranes. Example is PEG-coated liposome doxorubicin to lessen cytotoxicity and enhance anticancer medication delivery [60].

A polymeric drug delivery system, composed of repeating units of certain polymers, like chitosan, PLGA, and PEG. These DSSs can be altered to react to variations in pH or the production of ROS. For example, polyamine loaded in folate and ligands for the HIV Transcriptional Transactivator (TAT) encapsulated in doxorubicin. Inorganic nanoparticle drug delivery uses nanocarriers such as silica, magnetic, and gold nanocarriers. They can be modified for targeted distribution

and used to encapsulate drugs. Examples can be drug protection by functionalized silica nanocarriers. Magnetic nanocarriers guided by magnetic fields across the human body. Gold nanocarriers for photothermal treatment and imaging. Peptide Nanoparticle DDSs with linear or cyclic structures that target cell surface receptors. They can be produced organically or by using fragments of naturally existing protein. Lung cancer treatment with peptidomimetic EGFR ligand encapsulated in a cationic liposome. As, liposome coupled with Receptor-Interactive Peptide Linker (RIPL) to target cancer cells that overexpress [60].

## 2.9 Metal Oxide Nanoparticles: Silica Nanoparticles

Silica nanoparticles (SiO2-NPs) hold considerable promise in the field of emerging nanomedicine due to their minimal cytotoxicity, extremely small size (below 100 nm), and capacity for modification with biomedical molecules. Their structure is composed of Si-O-Si bonds, with hydroxyl groups (silanol, Si-OH) covering their surfaces. By incorporating molecules of organic matter and functional compounds into their structure, they obtain new functions, considerably extending their in vitro uses for bioimaging, biosensors, and in vivo applications such as cancer treatment and drug administration. The size of those nanoparticles is important to their usefulness in biological applications [61].

Silica nanoparticles exhibit a remarkable property, when applied to surfaces, they adhere to molecules, enabling the surfaces to repel dirt and water effectively. This property is utilized in materials like glass, tiles, wood, and stone, preventing dirt adhesion and facilitating easy removal of water and contaminants. Nano-silica also has uses in biology, including cell, a gene, and immune therapy. Additionally, delivery of drugs, photothermal treatment, biological analysis, bio catalysis, and biological engineering [62].

This study is going to utilize sodium metasilicate as source for silica nanoparticle synthesis, Due to its cost-effectiveness, biodegradability, and safety, sodium

metasilicate is chosen as the silicon source. This silicon is suitable for reactions in water-based environments, which saves time and reduces risks during synthesis. Thus, the synthesis approach developed and executed in this study will contribute new insights into the production of silica nanoparticles using sodium metasilicates as the source of silicon [63].

### 2.9.1 Structural Forms of Silica

Silica can be found in two structural forms, crystalline and amorphous. Crystalline particles like quartz, crystallite and tridymites have arranged in orderly and repeating patterns. On other side, amorphous material like opal lacks this orderly arrangement.

Naturally occurring silica can be both amorphous and crystalline form. Amorphous silica are the substances that are hyalite opal and natural-silica glass (Fig 2.7), and crystalline silica minerals like $\alpha$-quartz, $\alpha$-cristobalite, and $\alpha$-tridymite. It is important to note that amorphous silica can transform into crystalline forms by the help of thermal treatments.

Silica in its impure form can have mix of these phases, such as quartz and sandstone. When it comes to crystalline silica it includes a variety of polymorphic structures, each with distinct low-temperature ($\alpha$) form and high-temperature ($\beta$) form. These transformations are significant in geological processes; for instance, amorphous opal-A can convert to crystalline opal-CT under conditions of increasing temperature and pressure, often linked with organic matter transformation in sediments [64].

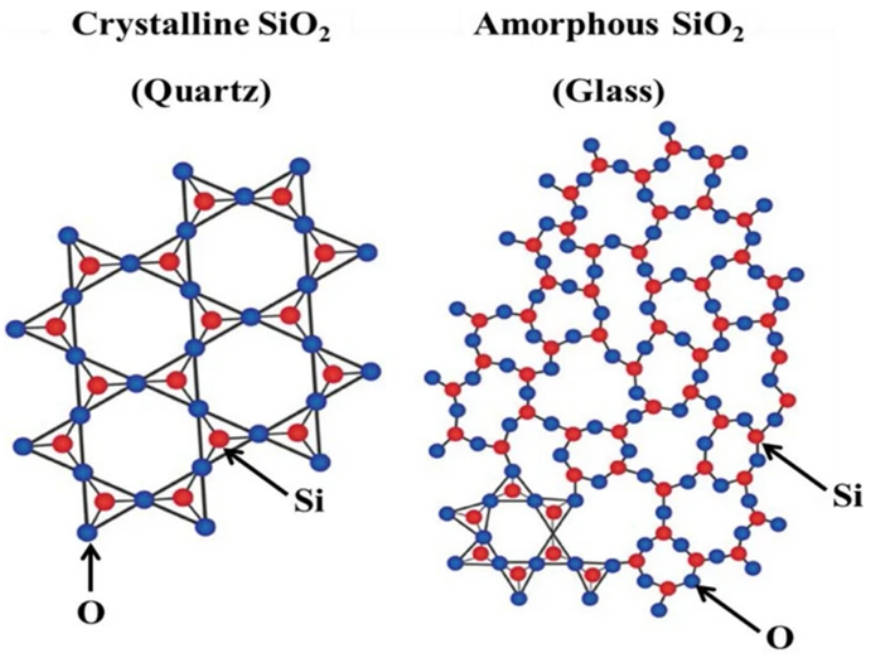


FIGURE 2.7: Structure of Silica, Crystalline and amorphous [64].

### 2.9.2 Synthesis of Silica-Based Materials

### 2.9.3 Chemical Synthesis

There are two synthesis techniques used mostly in chemical synthesis of silica nanoparticle:

- Chemical synthesis involves the technique called sol-gel technique that facilitates the production of pure, homogeneous silica materials in various forms like fibers, films, and submicron powders. It is also done for the transformation of the forms as colloidal sol-suspension into a 3D-interconnected gel network by the help of the hydrolysis and polymerization reactions process of metal alkoxides. Different methods of chemically synthesized nanoparticles are given in (Table 2.2) [65].
- Another method for silica nanoparticle synthesis is Stober method, in this low-temperature sol-gel as an approach can be used for synthesis (Table 2.2). The process involves the hydrolytic condensation reaction of Si–OH groups, replacing alkoxide groups (–OR) with hydroxyl groups (–OH). To make silica

nanoparticles from 100nm to few micrometers there is need of controlling precursor concentrations during hydrolysis, this includes various shapes such as nano-cubes and spheres [65]. For chemical synthesis, Tetraethyl Orthosilicate (TEOS) and ethanol concentrations can be considered to play a crucial role in determining size and distribution in silica-nanoparticles. Large particles are made when higher concentrations are used. The pH, reaction temperature, and duration influence particle size and morphology. Different types of surfactants are used like PEG, these help in controlling the size and help in preventing agglomeration. Silica nanoparticles synthesized via sol-gel methods find applications in nanomedicine and various industries [65]

TABLE 2.2: Represents chemically synthesized silica nanoparticles

| **Method** | **Observation** | **Reference** |
|---|---|---|
| Stober | In this, opals of silica opals with diameters 480 nm and 540 nm are formed. | [66] |
| | Particle sizes: 50 nm, 55 nm, 130 nm. Size increases with TEOS and NH3 concentrations. | [67] |
| Sono-chemical sol-gel process | Dispersed without agglomeration, average size of 9 nm, controlled by PEG 1000 surfactant. | [68]. |
| Sol-gel method | Average size ranges from 79.6nm to 87.3nm, 700$^o$C temperature was used to optimize calcination and 2h aging time. | [69] |
| Micelles entrapment approach | Particle sizes range from 28.91 nm to 113.22 nm, controlled by reaction temperature and solvents. | [70] |

#### 2.9.3.1 Silica Nanoparticles Synthesized by Green Synthesis

It is possible to produce green silica nanocomposites using sodium silicate and aloe vera gel. As, silica nanoparticles are synthesized using aloe vera gel as a green and sustainable source. Aloe vera gel serves as a biocompatible matrix rich in polysaccharides, facilitating the formation of silica-polysaccharides nanocomposites. This approach has helped in leverages the renewable nature of aloe vera but

also enhances the self-cleaning properties of solar mirrors due to the hydrophilic and adhesive characteristics of the polysaccharide-rich gel matrix [71].

Silica nanoparticles are synthesized from rice husk through an alkaline precipitation method. This process involves utilizing rice husk ash, a byproduct of rice processing, which is rich in silica. The ash is treated with an alkaline solution under controlled conditions, typically at pH 7 and a temperature of 90$^o$C for several hours. During this reaction, silica dissolves in the alkaline medium, forming a soluble silicate solution. Subsequently, under these conditions, silica nanoparticles gradually precipitate out of the solution. This method is considered environmentally friendly and economically feasible, utilizing a readily available agricultural waste product to produce nanoparticles that find applications across various fields including biomedicine, electronics, and environmental remediation [72].

### 2.9.4 Applications of Silica Nanoparticle

Nanoscale materials have garnered significant interest for their remarkable potential in diverse applications, offering unique technological advancements. Silica nanoparticles, in particular, are important in domains such as catalysts, delivery of medications, medicinal uses, environmental remediation, and treatment of wastewater (Fig 2.7). Their innovative properties promise to address numerous challenges across various scientific disciplines.

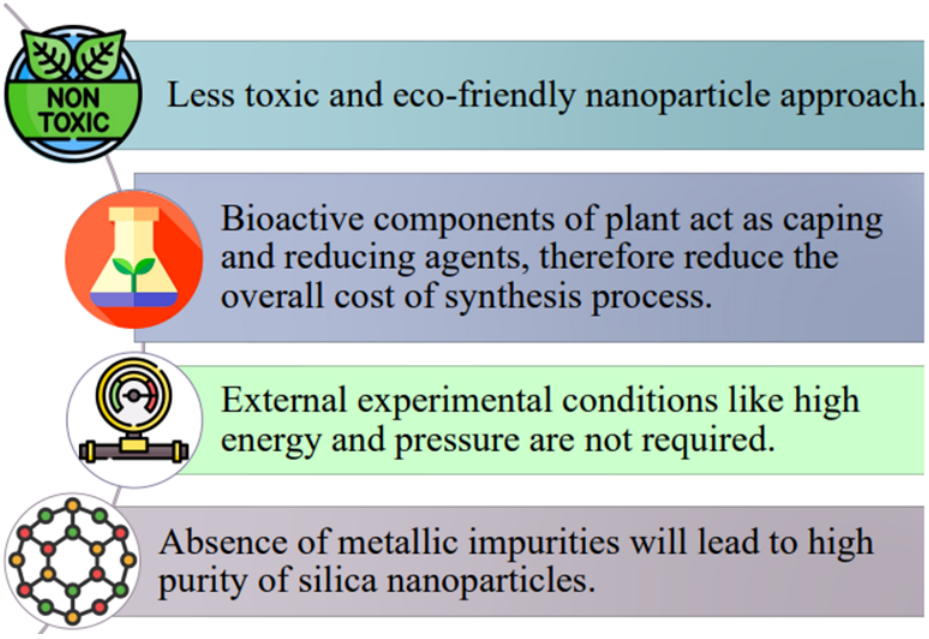


FIGURE 2.8: Green synthesized silica nanoparticle advantages [74].

Recent advancements in nanomaterials have sparked significant research interest in application od nanomaterials in biological sectors such as delivery of drugs, genetic therapy, and cancer treatment. MSNs offer unique advantages including their morphology, large pore size for drug reservoirs, and surface functionalization capabilities, enabling precise control over drug release [73]. MSNs are highly biocompatible and can target specific organs or tissues, making them promising carriers for therapeutic agents, including anti-cancer drugs and gene therapies [74].

Silica nanoparticles can be engineered to carry imaging agents (e.g., fluorescent dyes, contrast agents) for diagnostic purposes, enabling real-time monitoring of drug delivery and therapeutic response in cancer patients. By combining therapeutic and diagnostic capabilities, silica nanoparticles support theragnostic applications, where drug delivery and imaging functionalities are integrated into a single platform for personalized medicine.

Silica-based drug delivery systems protect encapsulated drugs from degradation, extending their shelf life and ensuring better stability during storage and transport. Silica nanoparticles are generally biocompatible and can be modified to enhance their biodegradability and reduce potential cytotoxicity, making them suitable for clinical applications. Silica nanoparticles can facilitate combination therapy by

delivering multiple drugs or therapeutic agents simultaneously, addressing heterogeneous tumors and overcoming drug resistance. The small dimension and surface characteristics of silica nanoparticles enable effective cellular absorption, which improves the efficacy of treatment of drugs given to cancer cells. Silica nanoparticles can be used in Photothermal Treatment (PTT) by absorbing Near-Infrared (NIR) light and turning them into heat, so selectively killing cancer cells while preserving healthy tissues. Functionalized silica nanoparticles can make cancer cells more sensitive to radiation treatment, increasing their efficacy and lowering the dose required [75].

TABLE 2.3: Silica nanoparticle application in cancer therapy as Drug carrier [75]

| **Type of cancer** | **Drug type** | **Functionalized material** |
|---|---|---|
| Bones | Doxorubicin (DOX) | PAA-capped MSNs |
| | Alendronate(AL) | Mesoporous bioactive glass (MBG) |
| | Doxorubicin(DOX) | Biodegradable hollow mesoporous-silica nanoparticles |
| Breast | Paclitaxel and curcumin | Lipid bilayer-coated with MSNs |
| | Doxorubicin(DOX) | MSN-coated with Au-nanorods |
| | Doxorubicin(DOX) | MSNs modified with arginylglycylaspartic acid peptide |
| Colon | CytC AS1411 | Nanoporous structure of porous silica nanocargo |
| | Doxorubicin(DOX) | |
| Liver | Sorefenib | Gold nano-shell MSNs |
| | Plasmid and CRISPR ribonucleoprotein | Lipid-coated mesoporous silica nanoparticle |

### 2.9.5 Toxicity/Safety of Silica Nanoparticle

Silicon-based materials are widely utilized across industries like construction, electronics, food, consumer goods, and medical fields, with applications ranging from bandages and lenses to dietary supplements and implants. Within nanotechnology, SiO2 NPs are valued for their size, surface area, biocompatibility, and minimal

toxicity. They play crucial roles in biomedical uses such as biosensors, drug delivery systems, and enhancing cellular uptake. Despite their potential benefits, concerns persist regarding the biocompatibility and safety of SiO2 NPs. While larger silicon materials are generally considered safe for human use, nanoparticles like silver and gold have demonstrated toxicity.

Studies examining SiO2 NPs have yielded diverse outcomes regarding their toxicity. Some in vitro research suggests SiO2 NPs can trigger inflammatory responses and apoptosis in specific cell lines, while other studies indicate minimal cytotoxicity. In vivo investigations have also produced conflicting results, with SiO2 NPs causing pulmonary inflammation and oxidative stress in some cases but showing no toxicity in others [76].

But also, SiO2 NPs offer high biocompatibility in vivo, as confirmed by numerous studies on toxicity, its biodistribution and excretion from the body. The FDA classifies silica as safe, commonly used in food additives and cosmetics. Silica particles disperse in soluble water orthosilicic acid (Si (OH)4), which accumulates as a minor element in humans. In vitro investigations reveal no toxicity at dosages up to 100 µg mL−1, and even greater quantities show low harm. However, crystalline silica nanoparticles may cause the development of ROS, thereby affecting cellular viability [76].

### 2.9.6 Precursors for Synthesis of Silica NP

Different salts or precursors can be used to synthesize silica nanoparticles, some of those are; sodium silicate (Na2SiO3), tetraethyl orthosilicate (TEOS, Si (OC2H5)4), sodium, metasilicate (Na2SiO3.9H2), potassium silicate (K2SiO3), silicon tetrachloride (SiCl4), silicic acid (H4SiO4).

Silica nanoparticles are synthesized from sodium silicate, which is produced in alkaline circumstances, sodium chloride (NaCl) serves as a crucial salt additive. NaCl plays multiple roles in this process: it acts as a precipitating agent, facilitating the controlled formation of silica nanoparticles by promoting their precipitation from sodium silicate solutions. Additionally, NaCl helps to stabilize the pH

of the reaction mixture, ensuring favorable conditions for nanoparticle formation and maintaining solution stability. The amount of NaCl also effects the size and shape of the silica nanoparticles generated, adding to the desired qualities of the end product. Overall, sodium chloride enhances the efficiency, yield, and purity of silica nanoparticles synthesized under alkaline conditions, making it an essential component in this nanoparticle fabrication method [77]. TEOS is used as a precursor in the solution-gelation inorganic polymerization process that produces silica nanoparticles. When TEOS interacts with water at the air-water interface, it hydrolyzes, progressively shedding ethoxy groups while enhancing the OH-stretch sign in sum-frequency generating (SFG) vibratory spectroscopy. Hydrolysis is followed by condensation, where Si-O- species form an interconnected network of Si-O-Si bonds, resulting to a reduction in the OH-stretch signal [78].

Sodium metasilicate is utilized as a precursor for synthesizing silica nanoparticles through fundamental chemical processes. Initially, during hydrolysis, water reacts with sodium metasilicate, producing silanol groups (Si-OH) and sodium hydroxide (NaOH). This reaction alters the pH of the solution and initiates the formation of silicic acid (Si(OH)4). Subsequently, in the condensation phase, silanol groups undergo further reactions, forming siloxane bonds (Si-O-Si) that link together to create the silica nanoparticle structure. These regulated reactions, affected by parameters such as temperature, pH adjustment, and solvent conditions, define the size, shape, and surface features of the resultant nanoparticles, which are critical for different applications spanning from medicine to materials science [79].

## 2.10 Significance of Medicinal Plants in World

The utilization of medicinal plants and herbal products is rapidly increasing worldwide due to the complexity of various pathologies and the adverse effects associated with synthetic drugs. Natural products have been extensively studied and confirmed to possess diverse pharmacological activities, including cytotoxic, antioxidant, antidiabetic, and antimicrobial. Moreover, its observed that the greater utilization of natural products is correlated with a reduced likelihood of major

health issues on a global scale, such as cancer, cardiovascular disorders, and type 2 diabetes. Consequently, the discovery of bioactive compounds from medicinal plants has garnered significant recognition within the scientific community [80].

### 2.10.1 Medicinal Plant Bioactive Compounds Significance

The bioactive compounds found in medicinal plants hold immense promise for managing diabetes effectively. From regulating blood sugar levels to mitigating diabetic complications, these natural remedies offer holistic solutions for individuals grappling with the challenges of diabetes. By integrating medicinal plants into diabetes management strategies, healthcare practitioners can empower patients to take control of their health and enhance their quality of life [81].

## 2.11 *Euphorbia milii*

FIGURE 2.9: Euphorbia milli plant aerial parts, Flowers and leaves [83]

It is a succulent shrub that climbs and can reach heights of up to 1.8 meters (5 feet 11 inches), characterized by densely spiny stems. The leaves primarily emerge from new growth and are oval-shaped, measuring up to 3.5 centimeters in length and 1.5 centimeters in width. Its small flowers are surrounded by noticeable

petal-like bracts, which can be red, pink, or white and reach diameters of up to 12 millimeters. The plant's sap possesses moderate toxicity [82].

*Euphorbia milii*, commonly known as "Christ thorn" or "Christ plant," and also popularly referred to as the crown of thorns, *Euphorbia milii*, as a medicinal plant found abundantly in tropical and subtropical areas [84].

*Euphorbia milii* Des Moul. (Euphorbiaceae), commonly known as an ornamental plant with wart-removing properties, *Euphorbia milii* is relatively less studied compared to other members of the genus. Prior to 2016, only 12 ingenol esters and 2 phorbol derivatives had been identified in *Euphorbia milii* However, recently there was uncovered 16 previously undescribed rosane-type diterpenoids from the aerial parts of *Euphorbia milii*, including two rearranged compounds featuring unique fused-ring systems (a novel 7/5/6 fused-ring system and a novel 5/7/5 tricyclic system, respectively). Intrigued by these novel structures, a systematic chemical investigation was initiated. This investigation led to the isolation of seven previously unreported diterpenoids, alongside nine known compounds, from the entire plants of *Euphorbia milii* [84].

### 2.11.1 Medicinal Properties

Studies have indicated that Euphorbia exhibits various medicinal properties, including anti-arthritis, anti-cancer, anti-convulsant, anti-inflammatory, anti-microbial, antioxidant, antispasmodic, anti-tumor, and antitussive effects, as well as benefits for hormonal regulation and myelopoiesis [85].

The early phytochemical screening of the methanol extract of *Euphorbia milii* indicated multiple positive bioactive components, including flavonoids, tannins, coumarin, and terpenoids, but no carbohydrates, alkaloids, glycosides, or steroids. These favorable bioactive components are remarkable because of their potential therapeutic applications. Flavonoids are well-known for their antioxidant and anti-inflammatory effects, making them useful in treating oxidative stress-related illnesses. Tannins have astringent and antibacterial characteristics, which can aid

in wound healing and infection prevention. Coumarins have anticoagulant, antibacterial, and anti-inflammatory properties, expanding their medical potential. Terpenoids are renowned for their anti-cancer, anti-malarial, and antiviral effects, which emphasize their importance in a variety of therapeutic scenarios. *Euphorbia milii*'s rich phytochemical composition highlights its potential as a source of bioactive chemicals for many purposes [86].

The phytochemical screening of the *Euphorbia milii* plant revealed an assortment of rich of bioactive components. The dried material contains high levels of flavonoids (20.3 ± 2.2 mg quercetin) and phenolics (3.61 ± 0.81 mg GAE). Compared to other species in the same family, is the highest among them. *Euphorbia milii*'s bioactivity is heavily reliant on flavonoids, a significant component. They are well-known for their powerful antioxidant qualities, which aid in free radical neutralization and oxidative stress reduction. This antioxidant activity protects cells from harm and may help prevent chronic illnesses like cancer and cardiovascular disease. Furthermore, flavonoids have anti-inflammatory, and anticancer effects, making them useful for a variety of medicinal applications [87].

The plant's latex, renowned for its mollusk-controlling effects, has been extensively utilized in traditional medicine. It has been historically employed to combat liver fluke and schistosomiasis in various animals, including sheep, cattle, and humans.

Several beneficial alkaloids, including $\beta$-sitosterol, euphol, euphorbol, euphorbol hexacosanoate, and the potent antileukemic macrolide lasiodiplodin, have been identified in the latex. However, detailed investigations into the latex's proteins and other biochemical constituents have been limited [88].

Euphorbia species exhibit a wide range of pharmacological activities, including anticancer, anti-viral, and antimicrobial effects. The latex of certain Euphorbia species has been traditionally utilized topically for treating skin ailments, sexually transmitted diseases like gonorrhea, migraines, and gastric parasites [89]

*Euphorbia milii* holds considerable medicinal significance within the genus because of that it has been traditionally employed for treating conditions like warts, cancer, and hepatitis. Additionally, *Euphorbia milii* exhibits antifungal, antinociceptive,

and molluscicidal properties. It has traditionally been utilized for its healing properties, such as promoting wound recovery, reducing inflammation, and exhibiting antimicrobial effects [89].

### 2.11.2 Traditional Uses and Therapeutic Potential

Euphorbia roots and tubers have gained recognition for their medicinal properties, particularly in Chinese traditional medicine. These botanical components serve as key ingredients in various Chinese herbal remedies [90].

### 2.11.3 Family and Distribution

With roughly 2000 species, the genus Euphorbia is a well-known angiosperm found around the world, mainly in Asia, Africa, Central and South America. From little annual or perennial herbs to sturdy wooden shrubs, vines, and trees, and succulent plants, Euphorbia species showcase remarkable variation in morphology. Notably, these plants are characterized by the production of a milky latex known for its irritant properties. Throughout scientific inquiry, the entirety of Euphorbia specimens, including their stems, leaves, latex, roots, and seeds, has been subjected to comprehensive chemical and pharmacological exploration [91].

The genus Euphorbia, belonging to the Euphorbiaceae family, stands as one of the largest genera of medicinal plants. It thrives across tropical regions, including countries like China and Pakistan [86].

### 2.11.4 Emerging Research

This plant has been helpful in production of eco-friendly silver nanoparticles (AgNPs) by utilizing the methanolic extract from the E. milii plant led to the creation of nanoparticles with remarkable antibacterial and enzyme inhibitory properties. These synthesized AgNPs demonstrated considerable effectiveness in inhibiting

the growth of S. aureus, showing greater activity compared to using the plant extract alone [92].

The emerging research of *Euphorbia milii* leaf extract is essential in the eco-friendly synthesis of zinc oxide (ZnO) nanoparticles. Bioactive compounds like flavonoids, tannins, phenolics, and saponins within the extract serve as reducing agents, converting zinc ions ($Zn_{2+}$) into ZnO nanoparticles. These compounds also stabilize the nanoparticles by capping them, preventing aggregation. Functional groups such as hydroxyl, carboxyl, and amino groups bind to the nanoparticles, enhancing stability. Additionally, the organic matrix provides nucleation sites for uniform growth. This method yields biocompatible ZnO nanoparticles suitable for biomedical applications [93].

# Chapter 3

# Research Methodology

The utilization of *Euphorbia milii* plant extract in the green synthesis of sodium metasilicate mediated silica nanoparticles for toxicity research is an intriguing concept that combines natural resources with nanotechnology.

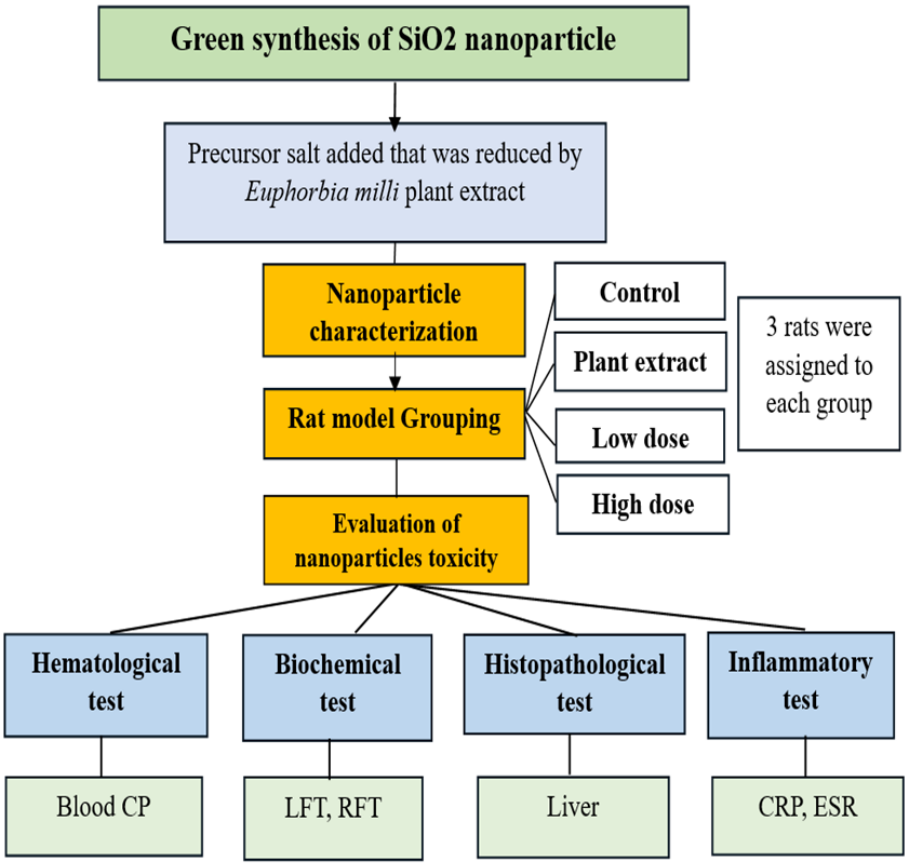


FIGURE 3.1: Methodology used during the study

## 3.1 Ethical Considerations

The ethical review committee of the Department of Bioinformatics and Biosciences, Capital University of Science and Technology, Islamabad, Pakistan, approved the research titled "*In Vivo* Toxicity Evaluation of Green Synthesized Silica Nanoparticles from *Euphorbia milii* in Sprague Dawley Rat Model" with reference number Ref# Sp24-BSBE-27.

All procedures followed the committee's guidelines to ensure the ethical treatment of the animals, with measures in place to minimize any discomfort or stress to the rats during the experiment.

## 3.2 Plant Collection and Extract Preparation

*Euphorbia milii* was sourced from the surroundings of Islamabad, the capital of Pakistan, during March 2024. The plant parts, including leaves and flowers, were identified and authenticated by the Botany Department of Arid Agriculture University, Rawalpindi.

Carefully selected leaves and flowers were collected and placed in a sterile storage box for transport to the laboratory. Fresh aerial parts were initially washed with distilled water to remove any surface contamination.

About 50g of the plant material was taken, cut into small pieces, and washed twice more to ensure cleanliness.

The cleaned plant material was added to 250 mL of distilled water in a conical flask and placed in a water bath maintained at 55-60$^{o}$C for 45 minutes to facilitate the extraction.

After extraction, the mixture was filtered using filter paper to obtain a clear, light yellow aqueous extract of *Euphorbia milii* (Fig 3.2) [95].


FIGURE 3.2: *Euphorbia milii* plant extract preparation.

## 3.3 Salt Solution Preparation

Sodium metasilicate [Na2SiO3] act as precursor salt that initiates the synthesis of silica nanoparticles. Here 0.5 M salt solution was prepared, in 20ml of distilled water 1 g of sodium metasilicate was dissolved.

Then this mixture was thoroughly stirred to make homogeneous solution, that ensuring complete dissolution of the salt. prepared 0.5M solution of sodium metasilicate was then used in the next steps for silica nanoparticle synthesized as precursor [95].

## 3.4 Silica Nanoparticle Synthesis

Silica nanoparticles were synthesized by using 20 mL of the .5M sodium metasilicate solution. this solution was added dropwise into 100 mL of the aqueous extract of *Euphorbia milii* while stirring continuously, resulted in 120ml of total solution volume. There was adjustment of the pH to 8-9 pH of the mixture by adding Sodium Hydroxide (NaOH) and Hydrochloric Acid (HCl) needed. The mixture was then heated to a temperature of 60-70$^o$C for 5 hours. During this period, a little jelly-like formation was observed, indicating the initiation of the reduction process. The color change from light yellow to deep brown further confirmed that the of silica nanoparticles were synthesized [95].

After the heating period, the mixture was allowed to cool to room temperature and was then centrifuged at 4000 rpm for 10 minutes. The obtained pellet was subsequently dried in an oven set at 80$^o$C to remove moisture. The dried material was washed twice with distilled water to eliminate any unreacted phytochemicals, followed by washing with ethanol to remove any residual salts [95].

Finally, annealing of the silica nanoparticle was done at 100$^o$C to transform the silica nanoparticles from brown to white, that helped in producing the final silica nanoparticle powder (Fig 3.3). This series of steps in (Fig 3.4), ensured the successful synthesis and purification of silica nanoparticles using a green synthesis method involving sodium metasilicate and *Euphorbia milii* extract [95].

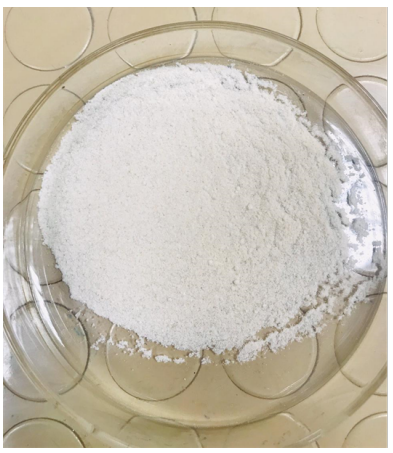

FIGURE 3.3: Silica nanoparticles ($SiO_2$ NPs) after washing and drying

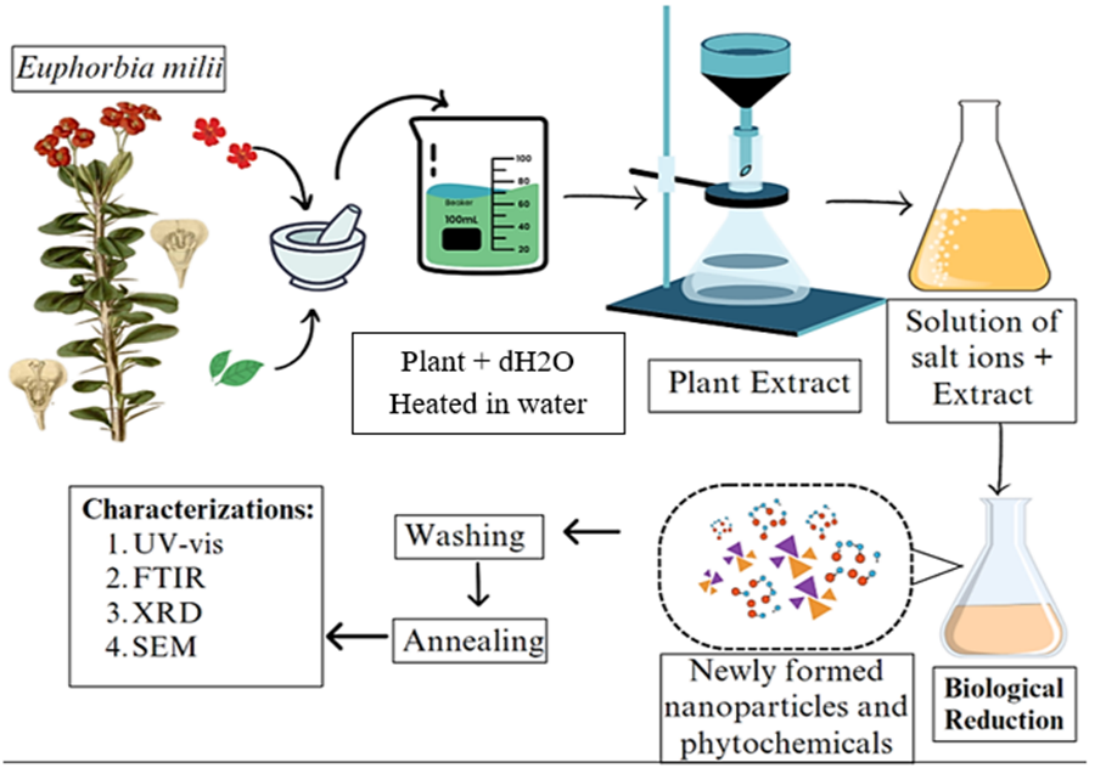


FIGURE 3.4: Schematic diagram of green synthesis of silica nanoparticles

## 3.5 Characterization of Nanoparticles

Characterization is important as the synthesis of NPs is occurring at nanoscale and hence, there is need to validate first that either the NPs have formed or not. There are various analytical techniques to characterize the synthesized nanoparticles: The characterizations techniques that are used UV-Vis spectrophotometry, FTIR, SEM and XRD.

UV-Vis spectrophotometry was utilized for analytical method employed for qualitative and quantitative analysis of chemical compounds/ elements [96]. Here this technique was used for validation purposes of silica NPs formation.

SEM is another technique used for morphological analysis of the shape and form of nanoparticles [97]. Chemical analysis using spectroscopic techniques by FTIR was done to confirm functional groups and chemical composition of plant extract samples as well was silica nanoparticles produced via green synthesis to know about their chemical nature [98]. For structural analysis XRD was done to identify

crystalline phases, that's a very versatile technique for analysis of nanoparticles, that has given information about structure of samples [99].

## 3.6 Experimental Animals Selection

Twelve adult male albino Sprague Dawley (*Rattus norvegicus*) rats 140-180gm, six to eight weeks old were taken from the Department of Pharmacy, CUST, Islamabad.

These rats were kept in typical stainless-steel cages with unrestricted access to water and fed a normal laboratory meal in an environment with regulated room temperature and 60–70% relative humidity [100].

## 3.7 Experimental Design

A total of 12 rats were randomly assigned to four groups (control, plant extract, low and high dose of $SiO_2$) each having 3 rats were designed and rats were kept in animal house for the period of 28 days (Fig 3.5). In the first week they were made to acclimatize to the animal house.

**Group 1-Control:** Rats in this group were provided with a standard diet and purified water for a period of 21 days.

**Group 2-Plant extract:** Rats received a daily dose of 150 mg/kg of dried extract solution combined with distilled water [101].

**Group 3-Low Dose Group:** Rats were given a low dose of 50 mg/kg of green-synthesized SiO nanoparticles via oral gavage, while continuing with a normal diet and purified water for 21 days [102].

**Group 4-High dose:** Rats were administered a high dose of 150 mg/kg of $SiO_2$ nanoparticles via oral gavage, alongside a regular diet and purified water for 21 days [102].


FIGURE 3.5: Sprague dawley rats were categorized into 4 groups in accordance with experimental design.

## 3.8 Dose Administration

Nanostructured $SiO_2$ NP suspended were administered in deionized water to the animals at doses of 50, and 150 mg/kg body on dry silica nanoparticle (Fig 3.6). For the 21 days of the experiment, the nanomaterial was given to the animals by gavage. Time of the dosing was same throughout the experiment.

TABLE 3.1: Low and high dose of silica nanoparticle measurement

| **Dose range of plant extract, low and high dose groups.** | | |
|---|---|---|
| Groups | Dose | Ref |
| Plant extract | 100mg/kg | [101] |
| Low dose | 50mg/kg | [102] |
| High dose | 100mg/kg | [102] |

FIGURE 3.6: Rats being given the dose with the help of feeding tube.

## 3.9 Body Weight

At the start of the experiment, all groups of rats, including the control and those treated with plant extract, low and high dose of silica nanoparticles synthesized using *Euphorbia milii*, were observed for their initial weights to establish a baseline for comparison. The weight of the rats were measured on regular bases, with the help of electronic balance (Fig 3.7), as morphological analysis for dosing date till the end of the study for 21 days [103].

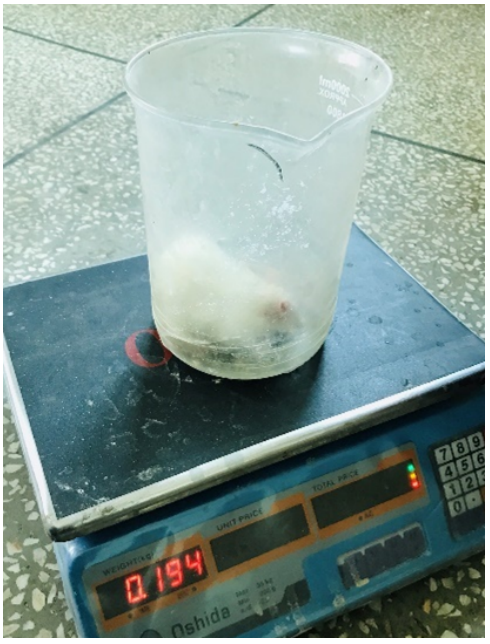


FIGURE 3.7: Rats body weight measuring

## 3.10 Animal Dissection and Blood Collection

On the 22nd day of the experiment, all rats underwent anesthesia using chloroform. To prevent contamination of blood samples were collected via cardiac puncture below the sternum for further biochemical analysis (Fig 3.8A). Following anesthesia, the rats were dissected (Fig 3.8B). A midline incision was made to access the abdominal cavity, ensuring minimal damage to surrounding tissues. The liver was carefully dissected out using standard dissection techniques, which involved gentle handling and precise cuts to preserve the organ's structure [104].

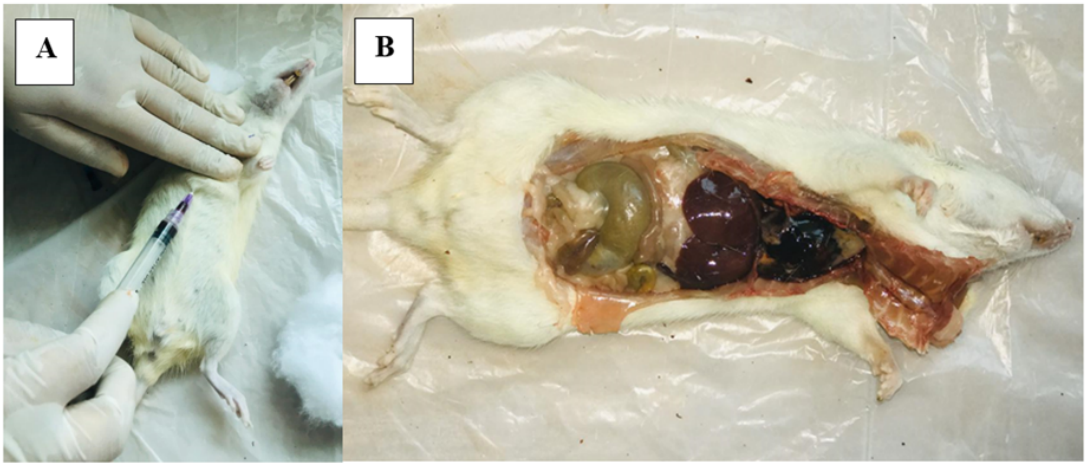


FIGURE 3.8: A. cardiac puncture for blood collection, B. Dissection of rat for liver extraction.

## 3.11 Hematologic Analysis

After the study period of 21 days, the hematological analyses of all the groups were conducted. The blood sampling of all the rats was done with the help of cardiac puncture and blood collected in Ethylenediaminetetraacetic Acid (EDTA) coated tubes containing disodium (5%) as in (Fig 3.9).

Blood parameters that were to be assessed with the help of an automated hematology analyzer were as follows: C-reactive Proteins (CRP), Erythrocyte Sedimentation Rate (ESR), Red Blood Cells (RBC), White Blood Cells (WBC), Hemoglobin (Hb), Mean Corpuscular Volume (MCV), Mean Corpuscular Hemoglobin (MCH), Mean Corpuscular Hemoglobin Concentration (MCHC), and differential leucocytes [103].

## 3.12 Biochemical Analysis

Blood sampling for serum biochemical examination was done after anesthetization as in (Fig 3.10). Thus, obtained serum was used to measure the following biochemical parameters, such as the Liver Function Test (LFT) and Renal Functioning Test (RFT), this helped to estimate all the biochemical parameters [103].

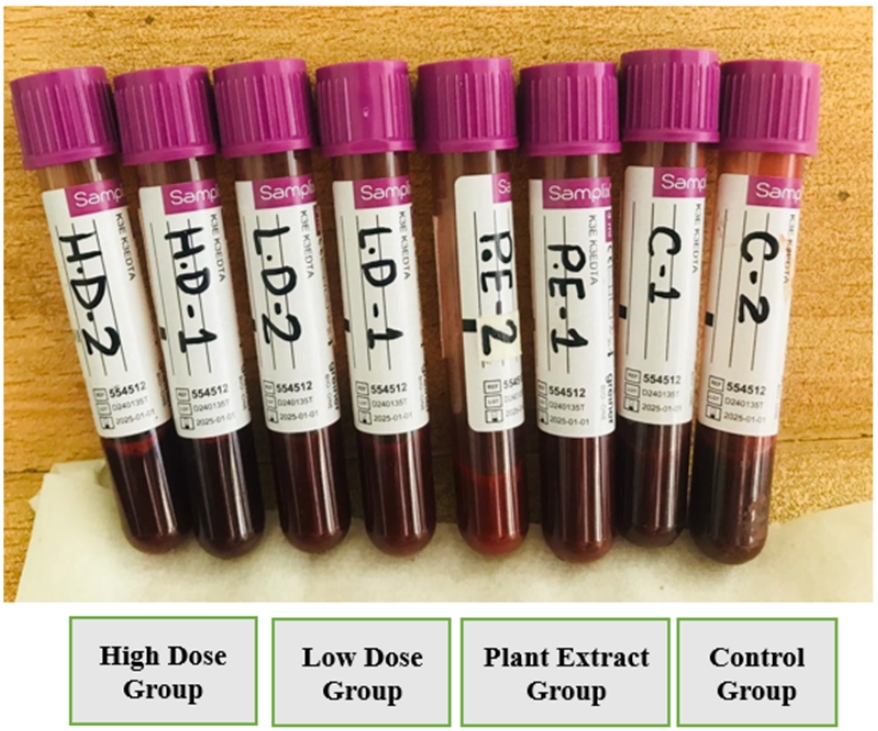


FIGURE 3.9: Blood samples collection for hematological analysis


FIGURE 3.10: Blood sample collection for biochemical analysis

## 3.13 Histopathology Study

Histopathology involves the microscopic examination of tissues, essential for diagnosing diseases and understanding structural changes. The animals were sacrificed for histopathological examinations. The liver of each rat was preserved in

10% formalin for histopathological analysis as in (Fig 3.11), in this study involving nanoparticles, examining liver tissue can reveal insights into their impact on organ health and function. Formalin fixation helps maintain tissue structure and prevents decay, ensuring the integrity of cellular morphology during microscopic examination [105].


FIGURE 3.11: Liver sample collection for histopathological analysis

## 3.14 Statistical Analysis

The study used three in-vivo tests and reported the results as Mean ± Standard Error of the Mean. To allow for multiple comparisons, one-way Analysis of Variance (ANOVA) was used, which helped with the statistical comparison of test samples to control groups. Duncan's multiple range test was also used to compare the means of various groups after ANOVA [106].

# Chapter 4

# Results and Discussion

## 4.1 Plant Extract & Silica Nanoparticle Synthesis

In this study, extract of *Euphorbia milii* plant was used to initiate the synthesis of silica ($SiO_2$) nanoparticles. The extract was prepared from the aerial parts of the *Euphorbia milii* plant in 100 ml of distilled water, followed by filtration that resulted in light yellow filtrate as shown in (Fig 4.1A). A 0.5 M sodium metasilicate ($Na_2SiO_3$) solution was prepared in 20 ml of distilled water and added dropwise to the plant extract. Bioactive compounds such as polyphenols and flavonoids in the extract acted as reducing agents, reducing the sodium metasilicate and forming silica nanoparticles. During this process, sodium ions ($Na^+$) were separated from silicate ions ($SiO_3^{2-}$), leading to the synthesis of silica nanoparticles. The successful production of nanoparticles was indicated by a color change from light yellow to deep brown (Fig 4.1B) as indicated in the study conducted previously [95]. Additionally, functional groups in the plant extract acted as stabilizers, preventing aggregation and maintaining the colloidal properties of the green synthesized $SiO_2$ nanoparticles [95].

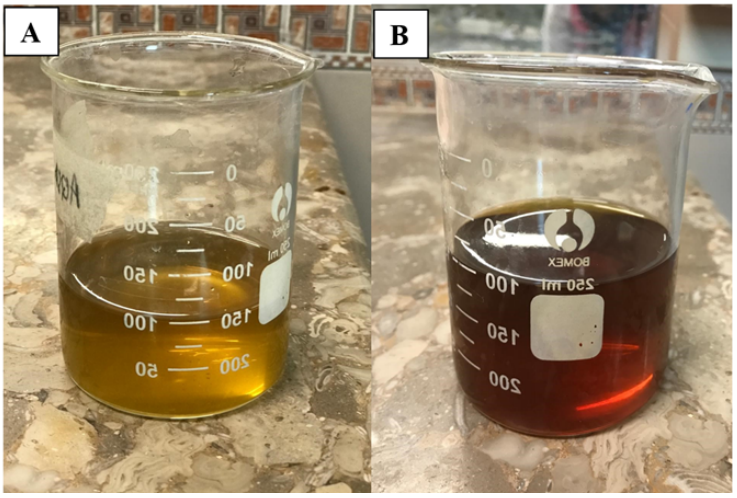


FIGURE 4.1: A. Synthesized extract of the *Euphorbia milii* plant, B. Color change indicated of plant extract when mixed with sodium metasilicate solution.

## 4.2 Characterization

Characterization of the $SiO_2$ nanoparticles is important and considered as the first step to confirm the synthesis amicably before its use for any desired application. The first indicator of synthesis of $SiO_2$ nanoparticles was the visual color change from yellow to deep brown.

The characterization of silica nanoparticles was done using different techniques like XRD to evaluate the green synthesis of the silica $SiO_2$ nanoparticle. FTIR for knowing about the biomolecules that bind and influence the formation and stability of synthesized nanoparticles. SEM-EDX to investigate the size and elemental composition of synthesized nanoparticles.

## 4.3 Fourier Transform Infrared Spectroscopy

FTIR is a very versatile tool because it allows scientists to study chemical reactions that have happened and to assist in detecting functional groups. FTIR spectroscopy also highlights the bonding properties of the nanoparticles. This information can provide details about the structure and chemical composition of the nanoparticle [107].

FTIR range was set at 400-4000 $cm^{-1}$, there was a baseline correction done with Origin Pro software. From the spectra results those peaks that correspond to Si-O-Si and Si-O bonds were identified. In the green synthesized silica $SiO_2$ nanoparticle FTIR results, it was clear that the bands nearby 3737 cm-1 in (Fig 4.2) was associated with the Si-OH, which is usually characteristic of the OH group corresponding to the available phytochemical of the *E. milii* plant extract that was OH group noted at 3215 $cm^{-1}$ peak in (Fig 4.3) [108].

The 2347 $cm^{-1}$ involves C-H stretching of $CH_2$ bonds, represents a carbon-rich surface in nanoparticle. C-O bending occurs at 1583 $cm^{-1}$ in (Fig 4.3) of nanoparticle , indicating carbon-containing functional groups. In addition, the band at 1531 cm-1 was due to the scissor bend and vibration of the water molecule $H_2O$ [109]. Peak vales from 400 to 1400 $cm^{-1}$ were important for the understanding of silica network formation because it covers Si-O-Si vibrations. Specific observations include 1060 $cm^{-1}$ that represents Si-O-Si asymmetric stretching lies between ∼1110 - 1070 $cm^{-1}$ as in (Table 4.1) and symmetric bending at 803 $cm^{-1}$ (∼815 - 790 $cm^{-1}$) of Si-O bonds [109]. Moreover, the band at 450 $cm^{-1}$ was represents the O-Si-O bending [110]. These vibrational spectra were essential for optimizing synthesis conditions to tailor silica nanoparticle properties for various applications.

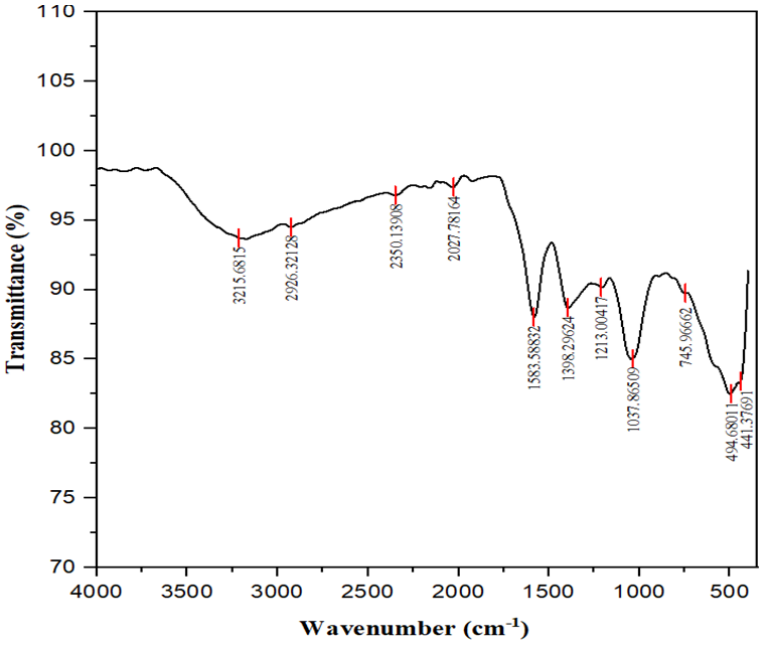


FIGURE 4.2: FTIR of the *Euphorbia milii* plant extract.

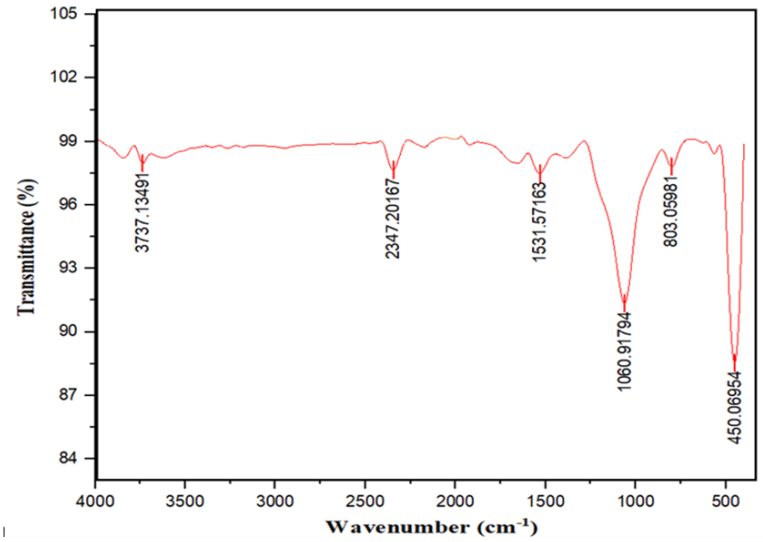


FIGURE 4.3: The FTIR of synthesized silica $SiO_2$ NPs.

Different functional groups that were present in the *Euphorbia milii* plant extract and silica nanoparticle were represented in the in the (Table 4.1) The peaks that present in the plant extract and silica nanoparticle represents different functional bonds in FTIR spectra, which denotes the reduction of the nanoparticles. These compounds were involved in the caping of the silica NPs, thereby it prevents aggregation.

TABLE 4.1: FTIR graph peaks value of plant and nanoparticle ranges.

| **Sr. No** | **Wavenumber Number (cm-1)** | **Frequency range (cm-1)** | **Functional group** | **Compounds** | **Ref** |
|---|---|---|---|---|---|
| 1 | 3737.1 (NP) | ∼3737 | Si-OH bonds | Hydroxyl compounds | [108] |
| 2 | 3215.6 (plant) | 3400–3200 | O-H group | Hydroxyl compound | [111] |
| 3 | 2926.1 (plant) | 3000-2840 | C-H stretch | C-H compounds | [112] |
| 4 | 2350.1 (plant) | 2355-2347 | C–H stretch | Symmetrical/ asymmetrical $CH_2$ bonds | [109] |
| 5 | 2347.2 (NP) | 2355-2347 | C-H stretch | C-H compounds | [109] |
| 8 | 1583.5 (plant) | 1650-1566 | C=C stretch | Cyclic alkene | [112] |
| 9 | 1531.57 (NP) | 1550-1500 | N-O stretch | Nitrogen compounds | [112] |

**Table 4.1 continued from previous page**

| Sr. No | Wavenumber Number (cm-1) | Frequency range (cm-1) | Functional group | Compounds | Ref |
|---|---|---|---|---|---|
| 10 | 1398.2 (plant) | 1440-1395 | O-H bending | Carboxylic compound | [112] |
| 11 | 1213.004 (plant) | 1275-1200 | C-O stretching | Alkyl aryl ether | [112] |
| 12 | 1060 (NP) | 1110 – 1070 | Si-O-Si asymmetric stretching | Si-O compound | [112]. [113] |
| 13 | 1037.86 (plant) | 1382-1036 | C-O bond | Carbon compounds | [113] |
| 14 | 803.05 (NP) | 815 – 790 | Si-O-Si symmetric bond | Si-O compounds | [112], [113], [114]. |
| 15 | 745.96 (plant) | ∼742 | C-Cl Stretch | Alkyl halide | [115] |
| 16 | 494.6, 441.3 (plant) | 490-620 | C-l stretch | Halo compound | [111] |
| 17 | 450.06 (NP) | ∼450 | O-Si-O bonds | Si-O compounds | [110] |

### 4.3.1 UV-vis Spectroscope

Ultraviolet–Visible (UV-Vis) spectroscopy is most used technique to explore the optical properties of the nanoparticle. UV-visible spectroscopy represents the absorbance spectra that is at visible range. It is represented in form of a plot of optical absorbance of wavelength [35].

The green synthesized Sio2 nanoparticle was further characterized by UV-visible spectrophotometer. The absorbance range was set from 200 to 700 nm. The absorbance peak was noted at 297nm wavelength (Fig 4.4), These results were in accordance with the study [116],as similar results were achieved. The strong absorbance of silica nanoparticle was observed between 250 nm to 300 nm [117]. Hence the highest peak at 297nm confirmed the presence of silica nanoparticles.

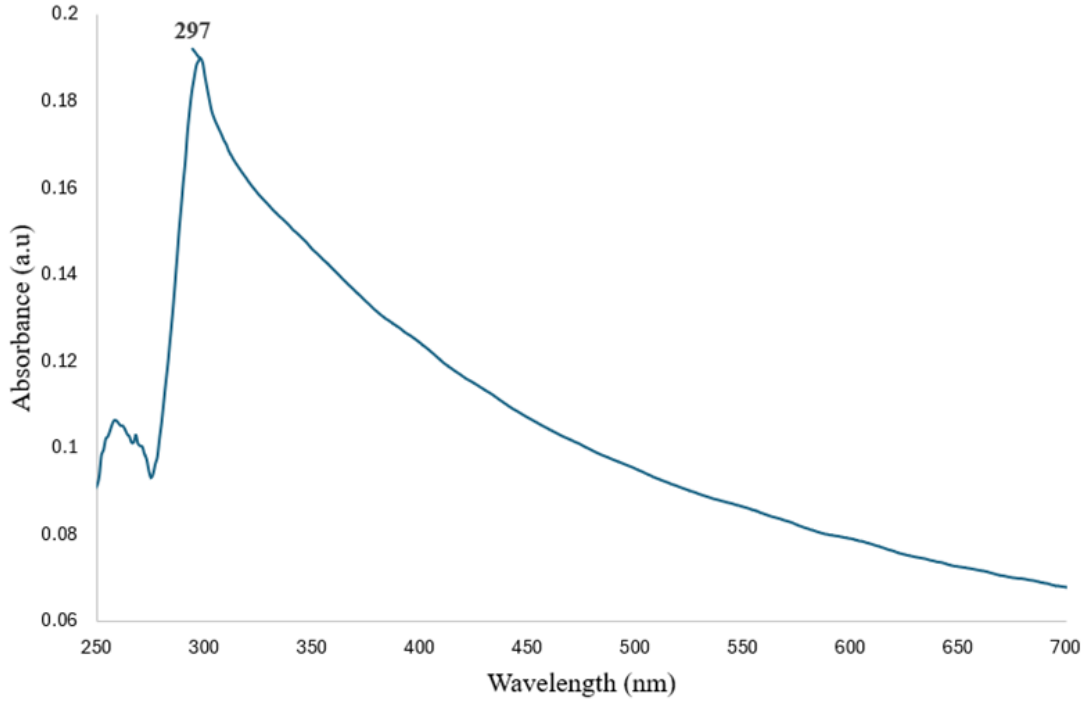


FIGURE 4.4: UV-vis spectrophotometer of green synthesized silica nanoparticle.

### 4.3.2 Scanning Electron Microscopy (SEM)

SEM was used to analyze the surface morphology of $SiO_2$ NPs that were green synthesized. SEM results, shown in Figure 4.5, represent that green synthesized $SiO_2$ NPs were polydisperse, meaning they differ in size, not like chemically synthesized $SiO_2$ NPs, which were uniform in size means monodisperse. The size of green synthesized silica nanoparticle ranges from nanoparticle 5nm to 21nm, as in Figure 4.5 [118]. The results were in accordance with study, reported that silica nanoparticle of such properties agglomerate. So, the green synthesized nanoparticles also tend to agglomerate/clump together, due to their larger surface area and the affinity they maintain during the dehydration process [119].

The phytochemicals in the plant extract used for green synthesis play a significant role in the stability and agglomeration of these nanoparticles. As a result, the $SiO_2$ NPs tend to stick to each other, forming irregular clusters [120].

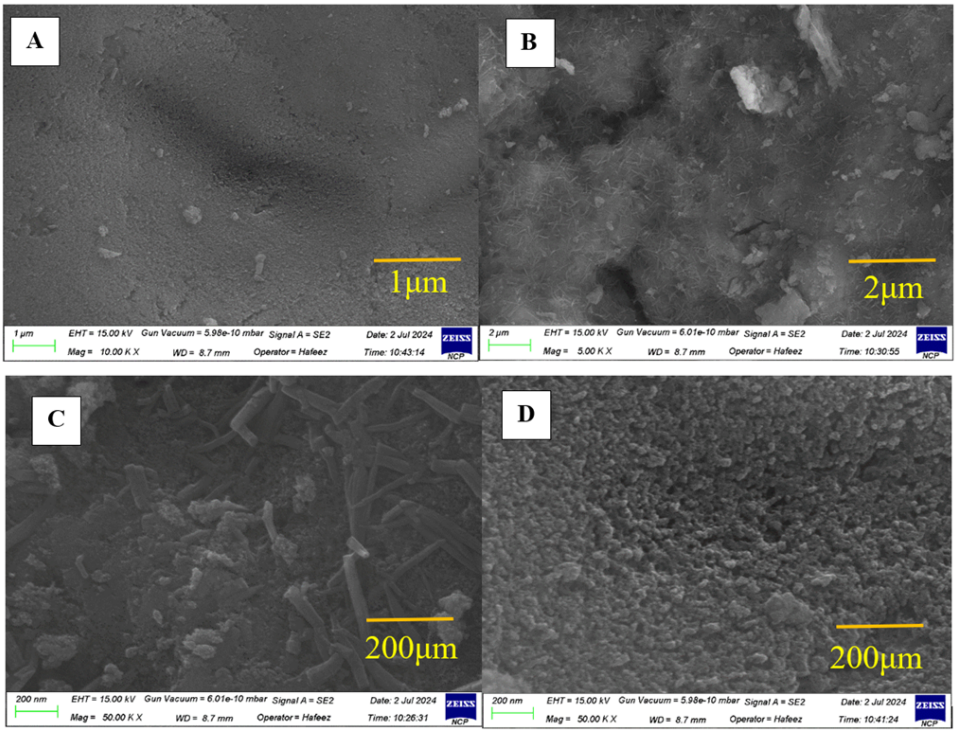


FIGURE 4.5: SEM images of green synthesized nanoparticles. A. 1$\mu$m at 10K X, B. 2$\mu$m at 5K X, C. 200$\mu$m and D) 200$\mu$m at 50 K X.

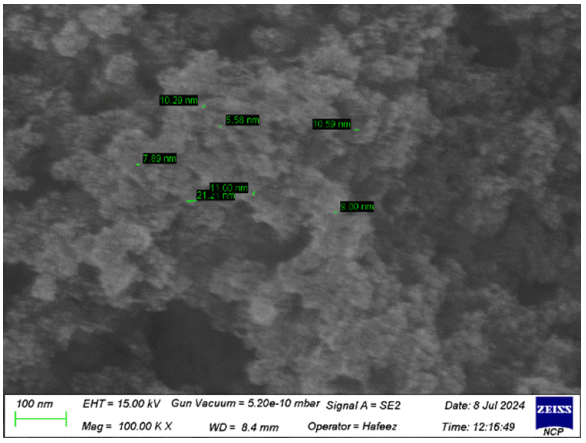


FIGURE 4.6: SEM results showed the size of silica nanoparticle that was from 5nm to 21nm size.

### 4.3.3 Energy-Dispersive X-Ray

The elemental composition of silica nanoparticles was confirmed using EDX spectroscopy EDX. Figure 4.7 displayed the EDX spectra of the samples. In the case of $SiO_2$ NPs, EDX analysis confirmed the presence of silicon (Si) and oxygen (O), constituting 70-78% of the composition. Minor Prescence of other elements

possibly from the precursor materials or experimental process were also detected indicated by additional signals such as carbon (C), calcium (Ca) and some trace elements like magnesium (Mg), and phosphorus (P). This comprehensive analysis via SEM and EDX supports the successful synthesis of the silica nanoparticle material [121].

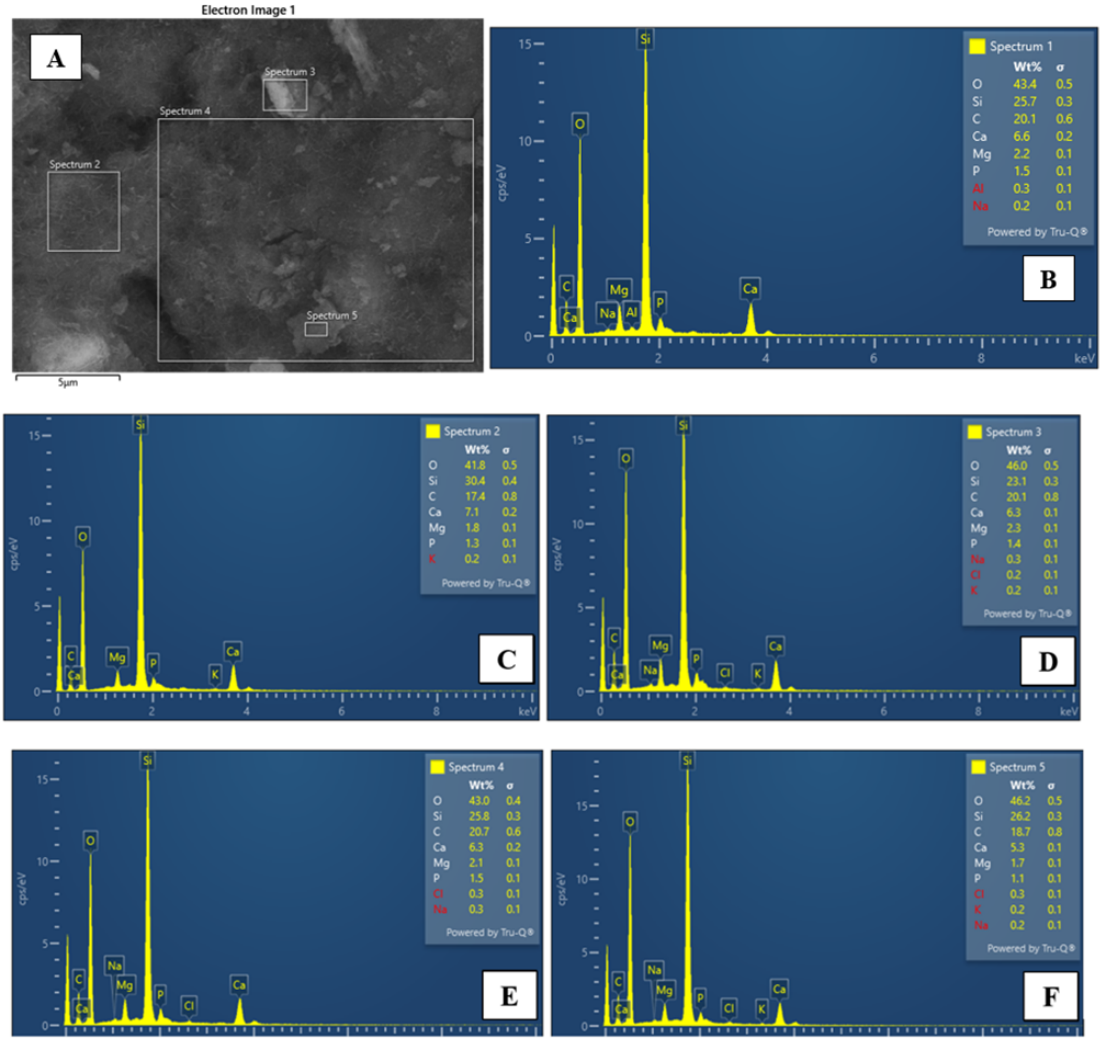


FIGURE 4.7: EDX results. A. 5 different spectrums shown. B-F. 1-5 spectrum results are demonstrated in form of graphs with a table of major to trace elements precent in the sample given.

### 4.3.4 X-Ray Diffraction (XRD)

XRD analysis of silica produced was performed on dry/ powder state of silica NPs. XRD resulted in the peak value of 22 degrees (Figure 4.8). These results are indication of the amorphous form of silica nanoparticles.

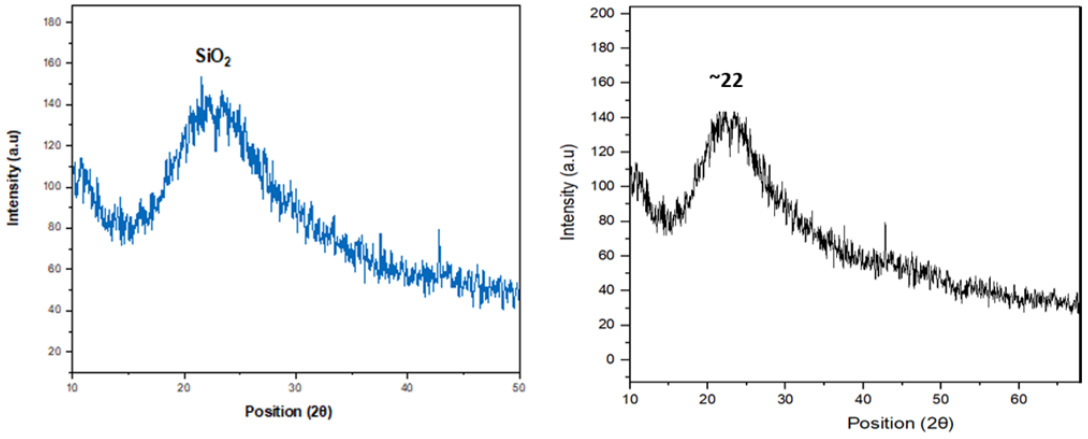


FIGURE 4.8: Diffraction pattern of silica nanoparticle obtained using XRD at the range of 10 to 80$^o$. The silica nanoparticle is found to be amorphous in shape.

SiO2 NPs have a peak range of 2 = 20 - 30 degrees, that was an indicator of amorphous silica nanoparticle synthesis [70]. This type of peak rose due to lack of long-range order in material that have amorphous form. These results also corelate to another study [122], where there was a broad peak observed that represents complete amorphous structure. There were no diffraction peaks observed except for a broad band centered at $\sim 22^o$ which was the characteristic peak range for amorphous $SiO_2$. nanoparticle.

## 4.4 Weight Assessment of Rats

At the start of the experiment, all groups of rats, including the control and those treated with plant extract, low and high dose of silica nanoparticles synthesized using *Euphorbia milii*, were observed for their initial weights to establish a baseline for comparison. Over the experimental period, the weights of the rats were regularly monitored and recorded to assess any potential toxic effects of the nanoparticle's morphological parameter. The initial average weights of the control group and the treated groups were comparable, ensuring that any observed differences could be attributed to the treatment.

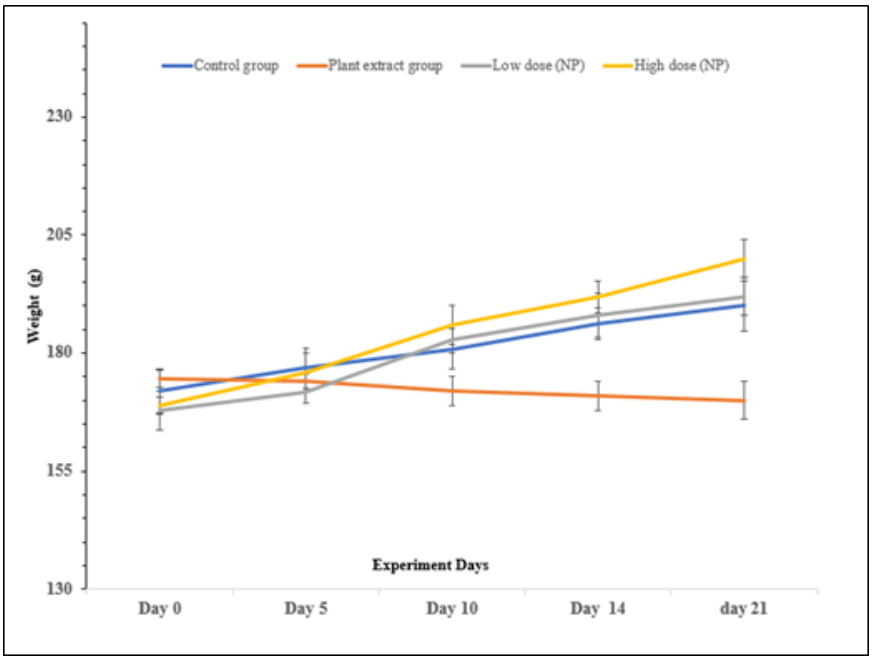


FIGURE 4.9: Graph showing weights of, control, plant extract only, low dose and high dose of $SiO_2$

TABLE 4.2: Weight, one-way ANOVA test measure the variance value, this the control, plant extract dose, low dose of $SiO_2$ (Np) and high dose of $SiO_2$ (Np).

| **Group Treatments (n=3)** | **Changes in body weight (g) at (days)** | | | | |
|---|---|---|---|---|---|
| | 0 | 5 | 10 | 14 | 21 |
| Control | 170.3±4.6a | 176±4.3a | 180.8 ±4.2a | 186 ±3.46a | 190.7±5.2a |
| Plant Extract | 174.6±1.8a | 174±1.6a | 172±3 a | 168.5 ± 3.1a | 166 ±4.7a |
| Low Dose $SiO_2$ (NP) | 167.8±4.1a | 172±2.3a | 184 ±3a | 190 ±4.6a | 192±.4a |
| High Dose $SiO_2$ (NP) | 168 ±1.8a | 176±4a | 188.6±4.1a | 194.5±3.4a | 200± 4a |
| P Value | 0.6 | 0.7 | 0.08 | 0.07 | 0.06 |

The silica nanoparticles were administered orally for 21 days. Changes in body weight recorded regularly. At the end of the study, no treatment-related death was detected. Body weight changes over the treatment period revealed no significant differences between the silica nanoparticle-treated and control groups (Figure 4.9).

The control group weight increased from 170 to 190g during the period of experiment. the plant extract group weight maintained slightly lower than control group from 174 to 166g, this may be due to plants bioactive compounds that have weight

lost activity [124]. The weight of low dose and high dose group animal increased from 167g to 192g and 168g to 200g respectively. The increase in weight of nano particle treated group compared to control group, showed insignificant results, as the increase in weight of low, high dose group and control group was at similar pace, as indicated in previous study [123].

## 4.5 Hematological Indices

Hematological tests are essential for assessing the overall health and detecting a wide range of disorders, including infections, anemia, and diseases related to blood and bone marrow. The results of hematological parameter identified in rats of control, plant extract, low dose and high dose group.

### 4.5.1 RBC and WBC

Red Blood Cells (RBCs) transport oxygen from the lungs to the body and return carbon dioxide to the lungs. White Blood Cells (WBCs) defend the body against infections and diseases. The plant extract group had (6.76.4±.5a) RBC levels and WBC counts was (5.6±1a) compared to the control group (Figure 4.10). These results were not significant, showing that the extract was not hazardous.

The study done with chemically synthesized silica nanoparticles, discovered that in RBC levels were reduced while WBC counts increased [125, 126]. These findings contradict the findings of current study, where both low and high dose of green synthesized silica nanoparticles resulted in rise of RBC levels while decrease in WBC counts compared to the control group (Figure 4.10).

However, these results were not significant enough to indicate toxicity as p-value was >0.05 (Table 4.3). This could demonstrate that silica nanoparticles derived from green production have no substantial harmful effects on RBC and WBC counts.

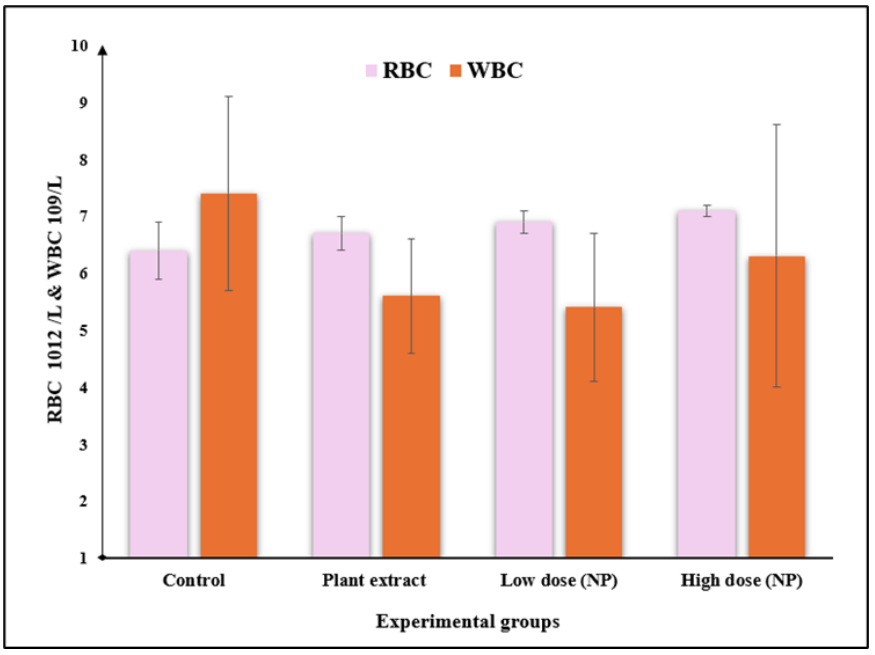


FIGURE 4.10: RBC and WBC graphical presentation in blood.

TABLE 4.3: RBC & WBC One-way ANOVA with in the control, plant extract dose, low dose of $SiO_2$ (Np) and high dose of $SiO_2$ (Np) along with mean ± standard error.

| **Parameters** | **Groups** | | | | **P Value** |
|---|---|---|---|---|---|
| | **Control** | **Plant Extract** | **Low Dose (NP)** | **High Dose (NP)** | |
| RBC (10^12/L) | 6.4±.5a | 6.7±.3a | 6.9±0.2a | 7.1±0.1a | 0.9 |
| WBC (10^9/L) | 7.4±1.7a | 5.6±1a | 5.4±1.3a | 6.3±2.4a | 0.8 |

### 4.5.2 Hemoglobin

Hemoglobin (Hb) is essential for oxygen transport in red blood cells, which aids in oxygen delivery to tissues and carbon dioxide elimination. In this study, Hb levels in the plant extract group increased slightly compared to normal values, but the increase was not statistically significant when compared to the control group as in Figure 4.11 and Table 4.4. These results were comparable with the study previously done [127], which found no significant increase in Hb levels regardless of dose. Another study reported that the study that *E. milii* latex did not cause teratogenic hazards or toxic effects in rats [124].

In contrast, control group compared to both low and high dosage nanoparticle (Figure 4.11), resulted exposure to nanoparticles increased Hb levels, indicating physiological stress caused by the nanoparticles. These findings are consistent with prior studies that also suggest that nanoparticle can induced physiological responses at some degree [124].

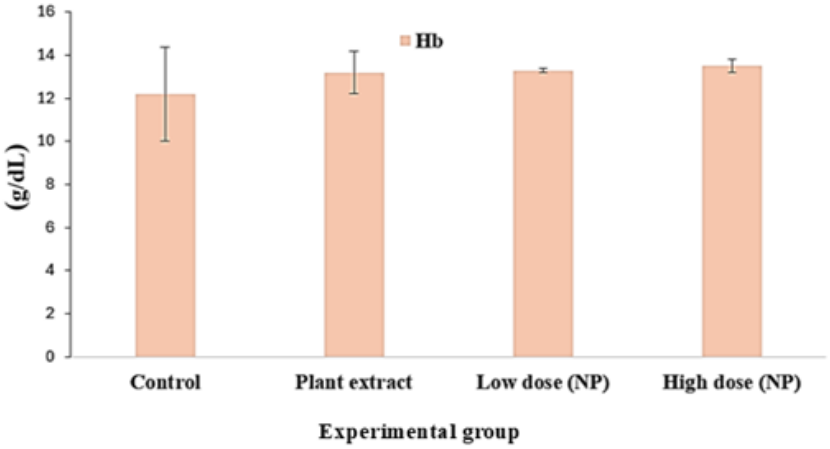


FIGURE 4.11: Hb levels graphical presentation in blood

TABLE 4.4: HB, one-way ANOVA test measure the variance value, the control, plant extract dose, low dose of $SiO_2$ (Np) and high dose of $SiO_2$ (Np) with mean standard error.

| **Parameters** | **Groups** | | | | **P Value** |
|---|---|---|---|---|---|
| | **Control** | **Plant Extract** | **Low Dose (NP)** | **High Dose (NP)** | |
| Hb | 12.2±2.2a | 13.3±1a | 13.5±0.1a | 14±0.3a | 0.8 |

### 4.5.3 MCV, MCH and MCHC

They are major indicators of hematological disorders. Mean Corpuscular Volume (MCV) MCV measures volume of a red blood cell on average, and results in showing anemias as microcytic, normocytic, or macrocytic. Mean Corpuscular Hemoglobin (MCH) indicates the average amount of hemoglobin per red blood cell, aiding in the evaluation of hyperchromic anemias. Mean Corpuscular Hemoglobin Concentration (MCHC) measures the concentration of hemoglobin in a given volume of red blood cells on average, providing insights into hemoglobin saturation

and hypochromic anemia. These parameters were considered crucial for understanding the underlying causes of various blood disorders [128].

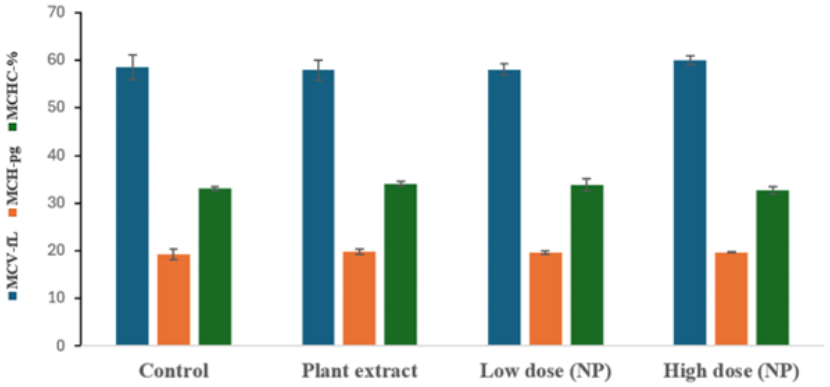


FIGURE 4.12: MCV, MCG, MCHC levels graphical presentation in blood.

TABLE 4.5: MCV, MCG, MCHC. One-way ANOVA with in the control, plant extract dose, low dose of $SiO_2$ (Np) and high dose of $SiO_2$ (Np) along with mean ± standard error.

| **Parameters** | **Groups** | | | | **P Value** |
|---|---|---|---|---|---|
| | **Control** | **Plant Extract** | **Low Dose (NP)** | **High Dose (NP)** | |
| MCV (fL) | 58.6±2.6a | 57.9±2.1a | 58±1.2a | 60.3±0.9a | 0.7 |
| MCH (pg) | 19.3±1.1a | 19.8±.5a | 19.6±0.4a | 19.7±0.1a | 0.9 |
| MCHC (%) | 33±.4a | 34.1±.4a | 33.9±1.3a | 32.7±0.7a | 0.5 |

The standard mean values of MCV, MCH, and MCHC showed no significant differences among groups (Table 4.5). Specifically, MCH values were 19.3±1.1 for the control group, 19.8±0.5 for the plant extract group, 19.6±0.4 for the low dose of green synthesized silica nanoparticles, and 19.7±0.1 for the high dose, all within normal ranges. The previous research aligns with the results of this study, which has shown consistent MCH values compared to controls in their rat model study [129].

The MCV values were similar across all groups (Figure 4.12), as 58.6 ± 2.6 for the control, 57.9 ± 2.1 for the plant extract group, and 58 ± 1.2 for the low dose nanoparticle group, with no significant differences observed. The high dose nanoparticle group had a slightly higher MCV of 60.3 ± 0.9, but with a non-significant p-value of 0.7 (Table 4.5). These findings indicate that neither the

plant extract nor the silica nanoparticles, at any dose, significantly affected red blood cell volume in rats [129].

The MCHC of the plant extract group showed a slight increase compared to the control, while the high dose nanoparticle group exhibited a slight decrease. The variability in the low dose nanoparticle group suggests potential effects on hemoglobin concentration. These results align with the toxicology report on SiO2, that has identified numerical differences of MCHC values under different silica nanoparticles concentrations show no Toxicological effects or animal model [130].

## 4.6 Liver Function Test (LFT)

Liver function tests (LFTs) provide valuable insights into the health and functionality of the liver. These tests measure various markers in the blood that indicate how well the liver is performing its essential functions, including liver enzymes like alanine aminotransferase (ALT) and aspartate aminotransferase (AST) measure the levels of these enzymes released by liver cells when they are damaged or stressed. Other tests are bilirubin, alkaline phosphates, total protein and albumin level counts. Interpreting LFT results requires consideration of these markers in conjunction with clinical symptoms and other diagnostic tests. Abnormal results may indicate various liver conditions, including hepatitis, cirrhosis, fatty liver disease, or drug-induced liver injury. LFTs are crucial for diagnosing liver diseases, monitoring treatment effectiveness, and assessing overall liver health [131].

### 4.6.1 Albumin and Globulin

Albumin is produced by the liver and is the most abundant protein in blood plasma. It helps maintain fluid balance and transports substances like hormones, vitamins, and drugs. Albumin keeps the right amount of fluid in blood vessels and carries essential molecules throughout the body. Low levels can indicate liver disease, malnutrition, or chronic inflammation. High levels are less common but can

be a sign of dehydration [132]. Globulins are proteins in blood plasma, such as alpha, beta, and gamma globulins. They are important for immune response, blood clotting, and transporting substances. Globulins help fight infections, clot blood, and carry metals and lipids. Low levels can suggest immune deficiencies, liver dysfunction, or kidney problems. High levels may indicate chronic inflammation, infections, or certain cancers [133].

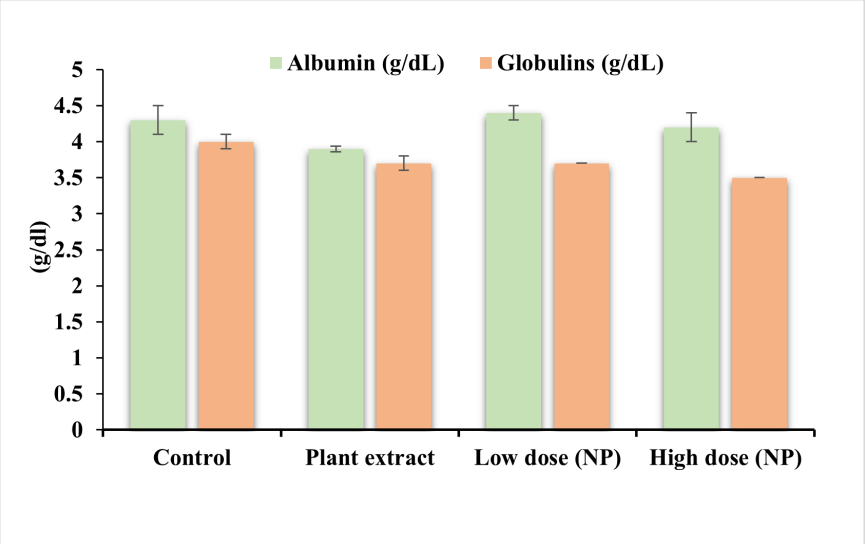


FIGURE 4.13: Albumin and Globulins graphical presentation in blood

TABLE 4.6: Al & Gl, One-way ANOVA with in the control, plant extract dose, low dose of $SiO_2$ (Np) and high dose of $SiO_2$ (Np) along with mean ± standard error, Duncan test.

| **Parameters** | **Groups** | | | | **P Value** |
|---|---|---|---|---|---|
| | **Control** | **Plant Extract** | **Low Dose (NP)** | **High Dose (NP)** | |
| Albumin (g/dL) | 4.3±.2a | 3.9±.04a | 4.4±.1a | 4.2±.2a | .4 |
| Globulins (g/dL) | 4±.1a | 3.7±.1ab | 3.7±0ab | 3.5±0b | .04 (Significant) |

The albumin levels within the experimental groups show no significant difference (p-value = 0.4) (Table 4.6). The control group has an albumin level of 4.3 ± 0.2 g/dL. The plant extract group has a slightly lower albumin level (3.9 ± 0.04 g/dL), but this is not statistically significant. The low dose nanoparticle group

has a slightly higher albumin level (4.4 ± 0.1 g/dL) compared to the control, and the high dose nanoparticle group has an albumin level of 4.2 ± 0.2 g/dL.

These variations are within the range of experimental error and do not suggest a significant impact of the treatments on albumin levels. According to study [125] the albumin values difference should be significant for the toxicity, the p-value > 0.05 also suggests there is no significant variance in results as compared to control values [125]. The results showed significant difference in globulin levels between the groups as p-value was 0.04. The control group has a globulin level of 4 ± 0.1 g/dL.

The plant extract group (3.7 ± 0.1 g/dL) and the low dose nanoparticle group (3.7 ± 0 g/dL) both show a slight reduction compared to the control. The high dose nanoparticle group has the lowest globulin level (3.5 ± 0 g/dL), indicating a significant reduction. This suggests that the treatments, particularly the high dose of silica nanoparticles, have a noticeable effect on globulin levels. t was suggested in prior research work, that when these were low albumin in the blood due to liver disorder then the globulin levels increase to balance the loss of albumin protein concentration in the blood to maintain the acceptable limits.

It was suggested in prior research work, that when these were low albumin in the blood due to liver disorder then the globulin levels increase to balance the loss of albumin protein concentration in the blood to maintain the acceptable limits [134].

### 4.6.2 Alkaline Phosphatase (ALP)

Alkaline Phosphatase (ALP) is an enzyme that occurs in whole body, in liver it is in high concentrations, along in bile ducts, and bones. It plays an important role in metabolizing proteins and is involved in processes such as bone mineralization and liver function. Elevated ALP levels can indicate liver disease and bone disorders. Conversely, low levels may be seen in certain genetic conditions or nutritional deficiencies.

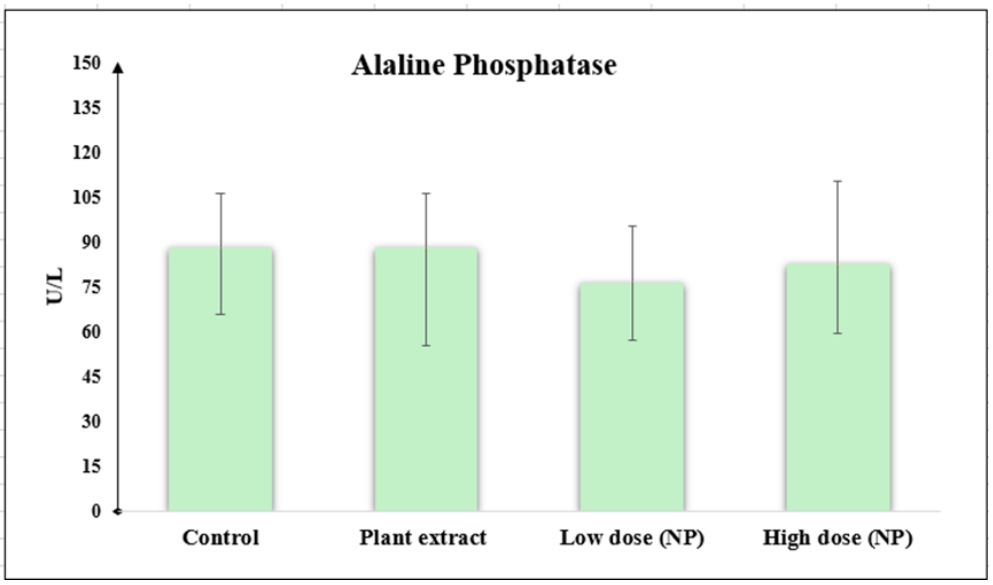


FIGURE 4.14: Alkaline phosphatase (ALP) graphical presentation in blood.

TABLE 4.7: ALP, One-way ANOVA with in the control, plant extract dose, low dose of $SiO_2$ (Np) and high dose of $SiO_2$ (Np) along with mean ± standard error, Duncan test.

| **Parameters** | **Groups** | | | | **P Value** |
|---|---|---|---|---|---|
| | **Control** | **Plant Extract** | **Low Dose (NP)** | **High Dose (NP)** | |
| Alkaline phosphatase (U/L) | 88±18a | 88±1a | 76.5±18.5a | 82.5±27.5a | .9 |

The results of low dose and high dose groups of green synthesized silica nanoparticles show that the ALP levels are not significantly high to be considered as toxic. Compared to the research done earlier, where acute toxicity was reported at 120 U/L (ALP), this value suggests that 76.5U/L and 82.5 U/L of low dose and high dose respectively in current study were not consider high enough to be toxic [125].

Then, mean values of extract-based results also when compared to control and silica nanoparticle administered groups treated with *Euphorbia milii* extract demonstrated normal ALP levels. This suggests that the extract beneficial effect and no toxic effects as well [124].

### 4.6.3 Alanine Aminotransferase (ALT) & Aspartate Aminotransferase (AST)

Serum biochemical parameters are vital for diagnosing diseases. Alanine Aminotransferase (ALT) is an enzyme in liver cells (hepatocytes) that helps convert L-alanine and -ketoglutarate into pyruvate and L-glutamate. Elevated ALT levels indicate liver cell damage. Aspartate Aminotransferase (AST) is found predominantly in liver and heart cells. Elevated AST levels can indicate liver damage or disease.

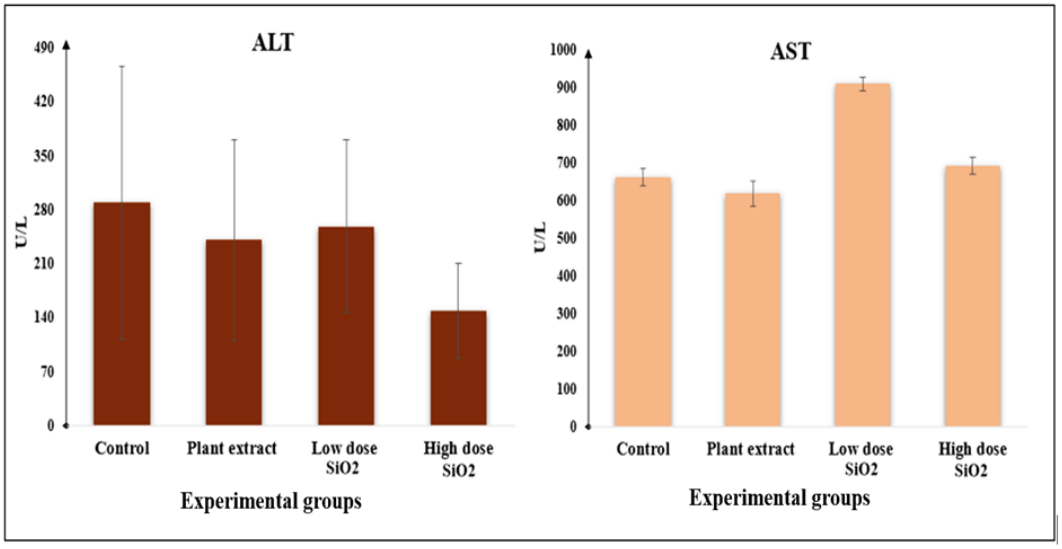


FIGURE 4.15: ALT and AST graphical presentation in blood.

TABLE 4.8: AST and ALP, One-way ANOVA with in the control, plant extract dose, low dose of $SiO_2$ (Np) and high dose of $SiO_2$ (Np) along with mean ± standard error, Duncan test.

| **Parameters** | **Groups** | | | | **P Value** |
|---|---|---|---|---|---|
| | **Control** | **Plant Extract** | **Low Dose (NP)** | **High Dose (NP)** | |
| ALT (U/L) | 289±177a | 240±129.5a | 258±112a | 148±61a | .8 |
| AST (U/L) | 661.5±2.5a | 617±33a | 907.5±19.5a | 690.5±236.5a | .4 |

During the experiment, group treated with *Euphorbia milii* extract has reduced ALT levels compared to the untreated control groups, suggesting a potential beneficial effect of the extract on liver health [124].

The ALT level in low dose of silica nanoparticles have low to no significant difference compared to control. But in high dose of 300mg/kg had high levels compared to control as represented in previous research [136]. In AST the silica nanoparticle given at low dose have low values compared to control and high dose have no significant difference in AST level compared to control that indicated green synthesized silica nanoparticles were safe. But in AST values of low dose is high compared to control group that means there are acute toxicity in the liver. Another study reported that, silica-based nanoparticles ALT and AST level increase compare to control group [136]. This suggested that in current study the level of ALT was not significantly high in low and high dose groups of green synthesized silica nanoparticles. Meaning there was no liver toxicity regarding ALT levels, but in AST the low dose of silica nanoparticles has shown an increased level, while high dose group of nanoparticles remain normal to the control group. This indicated low dose of nanoparticles might have caused some toxicity in liver that has released AST into the blood whereas high dose of silica has activated protective mechanisms, that have prevented further damage to liver resulting in lower AST levels.

### 4.6.4 Bilirubin

A waste product produced by the liver during the breakdown of old red blood cells. Elevated levels can indicate liver dysfunction or bile duct obstruction, in contract to the results in Table 4.9 and Figure 4.16 the bilirubin result was consistent and no change was observed in low dose and high dose of $SiO_2$ (NP), indicating no liver dysfunctionality.

TABLE 4.9: Bilirubin, One-way ANOVA with in the control, plant extract dose, low dose of $SiO_2$ (Np) and high dose of $SiO_2$ (Np) along with mean ± standard error, Duncan test.

| **Parameters** | **Groups** | | | | **P Value** |
|---|---|---|---|---|---|
| | **Control** | **Plant Extract** | **Low Dose (NP)** | **High Dose (NP)** | |
| Bilirubin Total (mg/dl) | 0.2±0.00 | 0.2±0.00 | 0.2±0.00 | 0.2±0.00 | - |

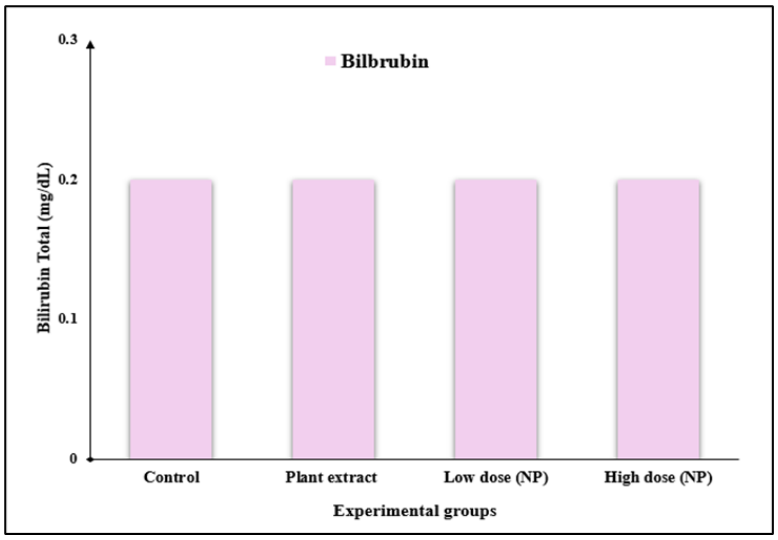


FIGURE 4.16: The Bilirubin graphical representation in blood.

## 4.7 RFT

RFT is a blood test used to know how well the kidneys are functioning. It tells important information about kidney cell damage. It includes measurements of Blood Urea Nitrogen (BUN) and serum creatinine. The high levels of BUN and creatinine may indicate kidney impairment.

### 4.7.1 BUN

BUN is a test that measures the amount of the nitrogen within the blood, that can be in form of protein metabolism, urea, or other waste product. As liver produces urea that is excreted by kidneys. Elevated BUN levels indicate impairment of the kidney and extreme low values indicate malnutrition or overhydration.

TABLE 4.10: Serum BUN, One-way ANOVA with in the control, plant extract dose, low dose of $SiO_2$ (Np) and high dose of $SiO_2$ (Np) along with mean ± standard error, Duncan test

| **Parameters** | **Groups** | | | | **P Value** |
|---|---|---|---|---|---|
| | **Control** | **Plant Extract** | **Low Dose (NP)** | **High Dose (NP)** | |
| Serum BUN (mg/dl) | 12±2.6a | 9.333±.9a | 12.9±2.6a | 7±1.4a | .3 |

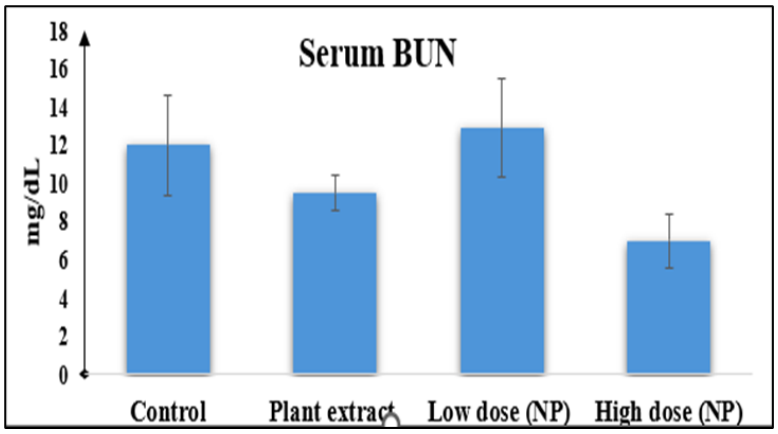


FIGURE 4.17: Serum BUN levels graphical presentation in blood.

It was observed that there were varying levels of BUN among different groups exposed to nanoparticles. The control group exhibited BUN levels of 12 ± 2.6 mg/dL (mean ± SD). The control group exhibited BUN levels of 12 ± 2.6 mg/dL (mean ± SD. The high-dose group showed significantly lower BUN levels of 7 ± 1.4 mg/dL, while the low-dose group exhibited BUN levels of 12.9 ± 2.6 mg/dL, indicating no substantial difference compared to the control. These findings suggest a dose-dependent effect of nanoparticles on renal function, with higher doses potentially affecting BUN levels differently compared to lower doses and the control group.

It was indicated in research [138], that mean values of the serum BUN lie in between the moderate range, which suggested green-synthesized silica nanoparticles may exert mild toxicity effect on renal function at higher doses, evidenced by lower BUN levels compared to the control group. However, at lower doses, the nanoparticles appear to have minimal acute effects on renal function based on BUN levels.

### 4.7.2 Serum Creatinine

It is the waste of muscles as they breakdown they make creatinine and a substance that occurs in muscles. Kidney helps to excrete out the creatinine from the body. So, measuring the levels of creatinine in the blood is crucial to know kidney health

and overall well-being. Elevated levels of creatinine indicate the dysfunction of kidney. That's why monitoring levels of kidney is important. In (Figure 4.18), current study was presented.

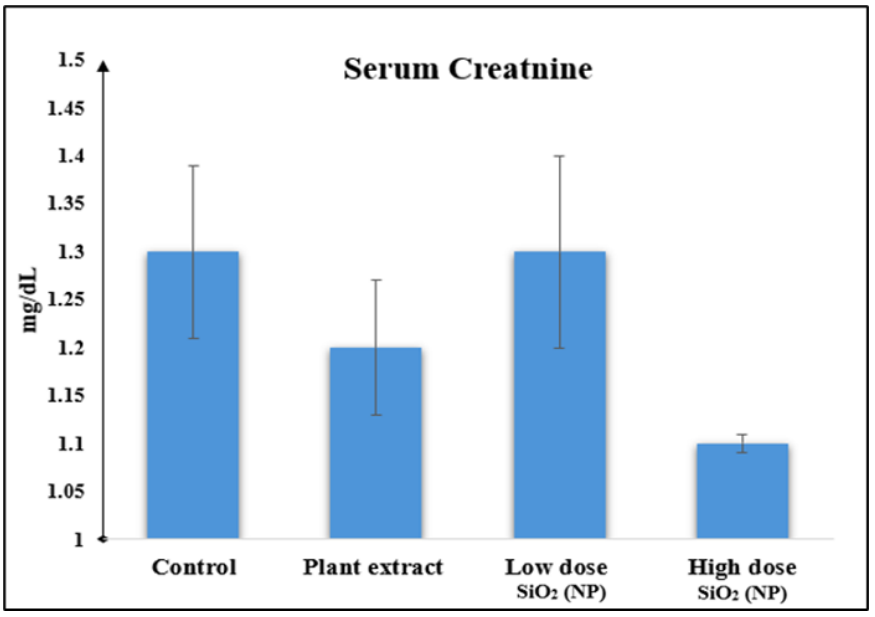


FIGURE 4.18: Serum Creatinine level. graphical presentation in blood.

TABLE 4.11: Serum Creatinine, One-way ANOVA with in the control, plant extract dose, low dose of $SiO_2$ (Np) and high dose of $SiO_2$ (Np) along with mean ± standard error, Duncan test.

| **Parameters** | **Groups** | | | | **P Value** |
|---|---|---|---|---|---|
| | **Control** | **Plant Extract** | **Low Dose (NP)** | **High Dose (NP)** | |
| Serum Creatinine | 1.3±0.09a | 1.2±.2a | 1.3±.1a | 1.1±.01a | .6 |

Results of serum creatinine showed that, the control group had level of 1.3 ± 0.09 mg/dL, the plant extract group had 1.2 ± 0.2 mg/dL, the low dose nanoparticle group had 1.3 ± 0.1 mg/dL, and the high dose nanoparticle group had 1.1 ± 0.01 mg/dL (Table 4.11). These results indicated that plant extract alone does not significantly impact renal function, as the creatinine levels in the plant extract group are similar to the control.

Also, the low dose nanoparticle group represent comparable creatinine levels to the control, suggested no significant renal function impact at low doses. Even at higher doses, the nanoparticles do not significantly impair renal function. These

results contradict with the previously documented research [139], that proposed silica nanoparticles cause significant increased creatinine levels in blood and cause toxicity. And other study on toxic levels of nanoparticles also supported the data [140].

The other research done on large silica nanoparticles showed similar results to this research as creatinine level in high dose of 300mg/kg are low. Where as in low dose the creatinine values are slightly high. It can be suggested that silica nanoparticle that are green synthesized showing such results can be considered safe [136].

## 4.8 CRP

C-reactive Protein (CRP) a protein produced by the liver in response to inflammation. It is a very sensitive marker for detecting acute and chronic inflammation in the body. Elevated levels of CRP in the blood indicate the presence of inflammation, which can be caused by infections, autoimmune disorders, or other inflammatory conditions. CRP levels rise rapidly in response to inflammatory stimuli, peaking within 48 hours as suggested [141].

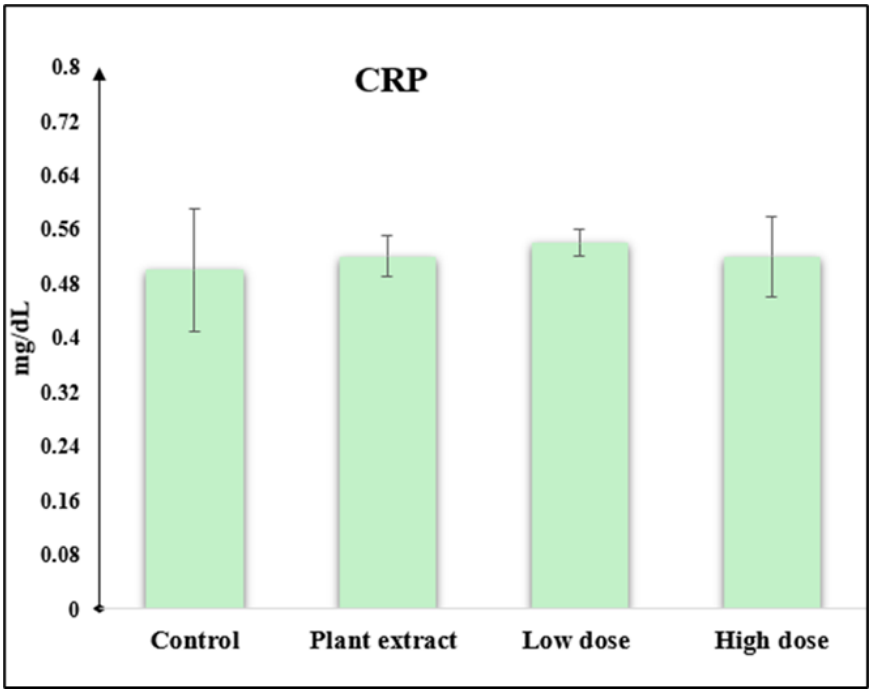


FIGURE 4.19: CRP levels graphical presentation in blood.

TABLE 4.12: CRP, One-way ANOVA with in the control, plant extract dose, low dose of $SiO_2$ (Np) and high dose of $SiO_2$ (Np) along with mean ± standard error, Duncan test

| **Parameters** | **Groups** | | | | **P Value** |
|---|---|---|---|---|---|
| | **Control** | **Plant Extract** | **Low Dose (NP)** | **High Dose (NP)** | |
| CRP mg/dL | 0.5±0.09a | 0.52±0.03a | 0.54±0.02a | 0.52±.06a | 0.97 |

CRP levels were measured in four experimental groups: the control group (0.5 ± 0.09), the group administered *Euphorbia milii* plant extract (0.52 ± 0.03), the low-dose silica nanoparticle group synthesized from green *Euphorbia milii* extract (0.54 ± 0.02), and the high-dose silica nanoparticle group (0.52 ± 0.06) as in (Table 4.12). The p-value of 0.97 suggests no significant difference in CRP levels among these groups, indicating that neither the plant extract nor the synthesized silica nanoparticles had a notable effect on systemic inflammation as measured by CRP.

A study done with chemically synthesized silica nanoparticle cause reactive oxygen species to increase in only 6 days of exposure, that was linked to CRP. Elevated ROS levels can reflect the presence of increased inflammation in the body, which was typically associated with higher CRP levels. These findings suggested that the green synthesized silica nanoparticles do not cause inflammatory response in the body [142].

## 4.9 ESR

Erythrocyte Sedimentation Rate (ESR) in rats, indicated rate of red blood cells settle in a vertical tube over a specific time, typically one hour [143]. This test served as an indicator of inflammation and is influenced by various factors like age, strain, and health status of the rats. In rats, high ESR typically shows inflammation or infection. It reflects increased blood protein levels causing faster red blood cell settling. And when there was low ESR levels normal physiological state or conditions affecting blood characteristics like sickle cell disease.

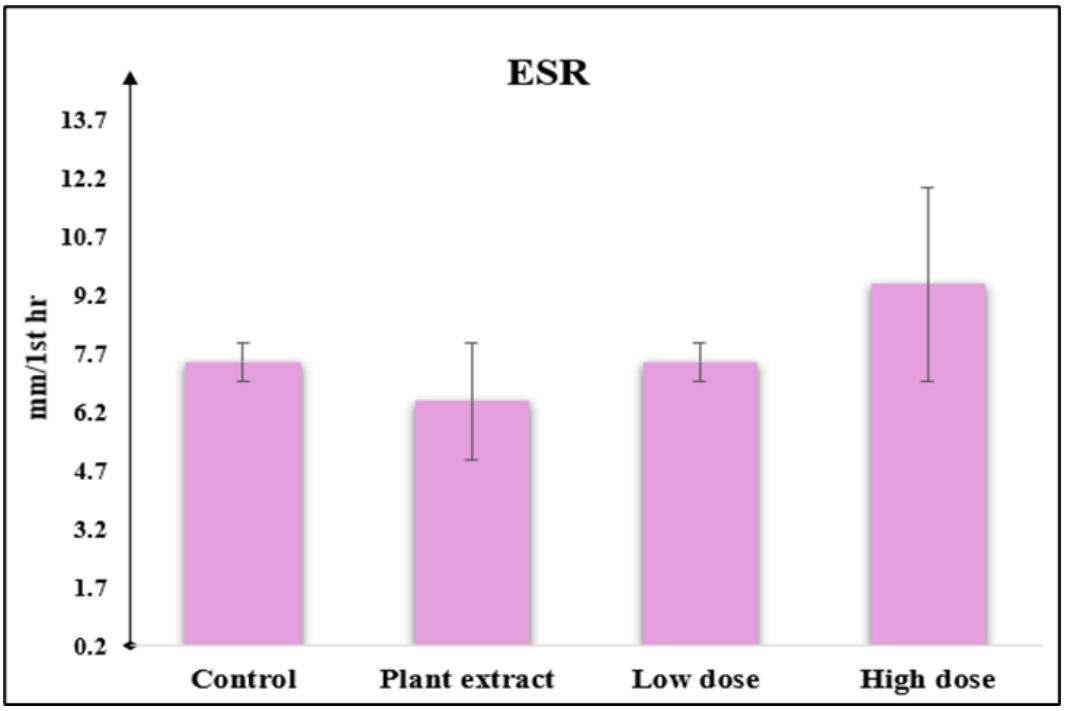


FIGURE 4.20: ESR levels graphical representation.in blood

TABLE 4.13: ESR, One-way ANOVA with in the control, plant extract dose, low dose of $SiO_2$ (Np) and high dose of $SiO_2$ (Np) along with mean ± standard error, Duncan test

| **Parameters** | **Groups** | | | | **P Value** |
|---|---|---|---|---|---|
| | **Control** | **Plant Extract** | **Low Dose (NP)** | **High Dose (NP)** | |
| ESR | 7.5±0.5a | 8.5±1.5a | 7.5±.5a | 9.5±2.5a | 0.7 |

The study investigated the effect of green synthesized silica nanoparticles from Euphorbia milii extract and Erythrocyte Sedimentation Rate (ESR) values in rats. Four experimental groups were examined as in (Table 4.13): a control group (7.5 ± 0.5), a group administered *Euphorbia milii* plant extract (8.5 ± 1.5), a low-dose silica nanoparticle group (7.5 ± 0.5), and a high-dose silica nanoparticle group (9.5 ± 2.5). P-value is >0.05 also suggests that the differences in ESR values compared to control was not significant, that was in accordance with the study done earlier [102]. The control and low-dose nanoparticle groups showed similar ESR levels, indicating minimal inflammatory response. In plant extract group exhibited change in ESR value, suggesting a mild to no inflammatory effect of the plant extract. As, study conducted previously [144], showed that the ESR

elevated levels are sign of inflammation in *Rattus norvegicus* that can be related to high dose that has increased the ESR level in blood, indicated that a pronounced inflammatory response possibly due to higher nanoparticle concentrations. These findings suggest varying degrees of inflammatory effects from low to high doses of silica nanoparticles in rats, underscoring the importance of dosage in nanoparticle toxicity studies.

## 4.10 Histopathology test

Liver is the largest solid organ in the body, that is primary site for nanoparticle accumulation and biotransformation of toxins. Numerous studies have shown that silica nanoparticles that are chemically synthesized can cause liver injury, including oxidative stress, inflammation, and metabolic disorders, potentially leading to fibrosis and liver failure [145]. The safety of silica nanoparticle is needed to be assessed. To evaluate the hepatotoxic effects of green synthesized silica NPs using Euphorbia milii extract, histopathological examination of liver tissues from exposed rats was conducted [145].

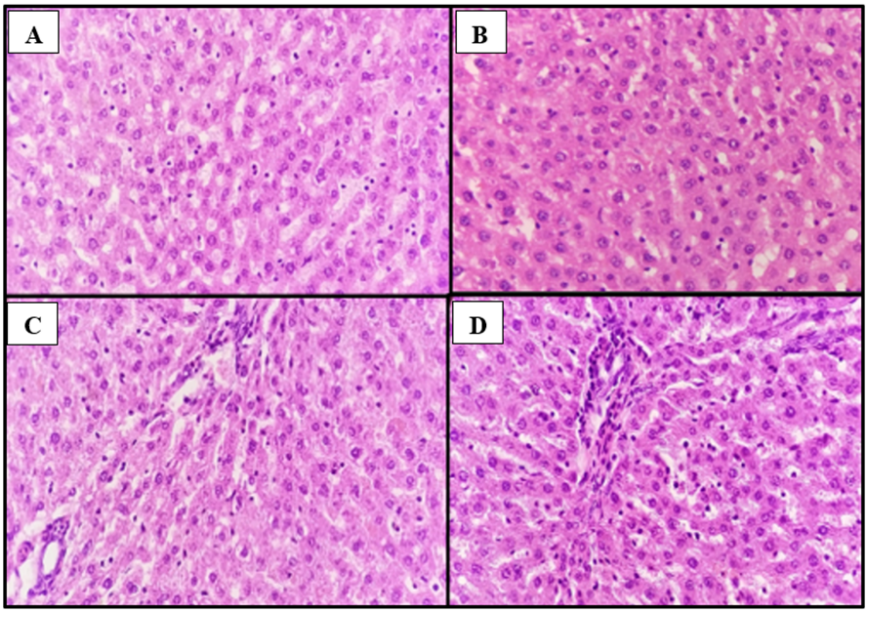


FIGURE 4.21: Liver histopathology test results A. Control, B. Plant extract, C. Low dose NP, D. High dose NP.

It was observed that the control group had normal uniform hepatocytes, with clear cytoplasm and prominent nuclei, overall normal cell morphology in (Figure 4.21A). In control group sinusoids were well defined and there were no apparent inflammatory cells or signs of necrosis. The (Figure 4.21A) represents healthy liver tissues. This serves as a baseline comparison for assessing the impact of silica nanoparticles. Liver sections from the plant extract-treated group (Figure 4.21B)showed similar results as the control group, with slight variations in cell size but overall uniform appearance. No significant sign of inflammation or necrosis observed. The liver section of plant extract group rats indicates also healthy or mildly affected liver tissues [146].

In low dose nanoparticles (Figure 4.21, C), there was slight damage to cells with the formation of interlobular fibrous bridges. In the low dose group, hepatocyte's structure is less uniform with some disruption. There might be mild infiltration of inflammatory cells, as show slight fibrosis there is minimal cellular damage observed. In high dose of silica nanoparticles group (Figure 4.21, D), there was damage observed with the formation of slightly larger interlobular fibrous bridges, affecting hepatic cords and sinusoids was observed. The high dose group of silica nanoparticles shows pronounced damage to liver cells and structures as compared to low dose of nanoparticles group. Noticeable disruption of hepatocytes arrangement with increased cell size variation, potential sign of starting of necrosis, and presence of inflammatory cell [146].

In summary, these observations illustrate the dose-dependent effects of green synthesized silica nanoparticles on liver tissue, ranging from normal morphology in the control to increasing damage and structural alterations in the low and high dose groups., whereas plant group showed minimal changes to healthy liver tissues. These findings are crucial for understanding the safety profile and potential risks associated with the use of silica nanoparticles in biomedical applications.

# Chapter 5

# Conclusion and Future Perspective

In conclusion, this research has explored the journey from green synthesis of silica nanoparticles using *Euphorbia milii* extract to their thorough characterization and subsequent in vivo toxicity assessment. By adopting eco-friendly synthesis methods, this research helped to addressed the growing need for sustainable nanoparticle production, aiming to reduce environmental impact and enhance biocompatibility for biomedical applications. Silica NPs were made by green synthesis approach have particle ranged in size from 5 to 21nm. They had amorphous structure and spherical shape this was characterized by using techniques such as SEM, UV-vis spectrum EXD, XRD, and FTIR have provided detailed insights into the structural and chemical properties of these silica nanoparticles, ensuring their integrity and suitability for various uses.

The in-depth evaluation of nanoparticle toxicity in rat models, notably albino Sprague Dawley rats, has been pivotal in determining their safety profile. The final results show that silica nanoparticles, when green synthesized and utilized at moderate amounts, can be more beneficial compared to higher amounts. Histopathological examinations, biochemical analyses, and systemic assessments have elucidated potential impacts on biological systems, emphasizing the importance of rigorous safety testing in nanomaterial development. This integrated approach

underscores the significance of balancing innovation with safety considerations, paving the way for responsible advancements in silica nanoparticle research and application across biomedical and environmental fields.

To build on these findings, several future research directions are recommended. Extended toxicity studies are needed to assess the long-term effects and potential accumulation of silica nanoparticles in various organs. Investigating the molecular mechanisms behind the changes in globulin levels will provide deeper insights into their impact on immune function. Expanding the research to include different animal models and eventually human trials will help confirm the safety and efficacy of these nanoparticles. Additionally, exploring the biomedical applications of these nanoparticles, such as in drug delivery and imaging, is promising due to their biocompatibility and unique properties. Finally, assessing the environmental impact of the green synthesis process and the nanoparticles themselves is crucial, considering the growing concern over nanomaterial pollution. This study significantly contributes to the field of nanotoxicology and nanomedicine, demonstrating the potential of plant-based green synthesis methods for producing biocompatible nanoparticles. The findings support further research and development, potentially leading to innovative applications in healthcare and environmental sustainability.

# Bibliography

[1] V. Singh, P. Yadav, and V. Mishra, "Recent Advances on Classification, Properties, Synthesis, and Characterization of Nanomaterials," in Green Synthesis of Nanomaterials for Bioenergy Applications, pp. 83–97, 2020.

[2] S. Ying et al., "Green synthesis of nanoparticles: Current developments and limitations," Environmental Technology & Innovation, vol. 26, p. 102336, 2022

[3] H. Moulahoum et al., "Emerging trends in nanomaterial design for the development of point-of-care platforms and practical applications," Journal of Pharmaceutical and Biomedical Analysis, vol. 235, p. 115623, 2023.

[4] A. Dhaka, S. C. Mali, S. Sharma, and R. Trivedi, "A review on biological synthesis of silver nanoparticles and their potential applications," Results in Chemistry, vol. 6, p. 101108, 2023.

[5] A. Mahendiran, N. Gopal, N. Duraisamy, and R. Rajamani, "A Comprehensive Literature Review on Pharmacological effects of Euphorbia milii (Crown of Thorns)," Advance Pharmaceutical Journal, vol. 8, no. 4, pp. 94–107, 2023.

[6] N. Joudeh and D. Linke, "Nanoparticle classification, physicochemical properties, characterization, and applications: a comprehensive review for biologists," Journal of Nanobiotechnology, vol. 20, no. 1, 2022.

[7] V. Selvarajan, S. A. O. Obuobi, and P. L. R. Ee, "Silica Nanoparticles—A versatile tool for the treatment of bacterial infections," Frontiers in Chemistry, vol. 8, 2020.

[8] N. S. Alharbi, N. S. Alsubhi, and A. I. Felimban, "Green synthesis of silver nanoparticles using medicinal plants: Characterization and application," Journal of Radiation Research and Applied Sciences, vol. 15, no. 3, pp. 109–124, 2022.

[9] N. G. Khlebtsov and L. A. Dykman, "Optical properties and biomedical applications of plasmonic nanoparticles," Journal of Quantitative Spectroscopy & Radiative Transfer/Journal of Quantitative Spectroscopy & Radiative Transfer, vol. 111, no. 1, pp. 1–35, Jan. 2010.

[10] D. Guo, G. Xie, and J. Luo, "Mechanical properties of nanoparticles: basics and applications," Journal of Physics. D, Applied Physics, vol. 47, no. 1, p. 013001, Dec. 2013.

[11] G. Priyadarshana, N. Kottegoda, A. Senaratne, A. De Alwis, and V. Karunaratne, "Synthesis of Magnetite Nanoparticles by Top-Down Approach from a High Purity Ore," Journal of Nanomaterials, vol. 2015, pp. 1–8, Jan. 2015.

[12] J.-H. Shim, B.-J. Lee, and Y. W. Cho, "Thermal stability of unsupported gold nanoparticle: a molecular dynamics study," Surface Science, vol. 512, no. 3, pp. 262–268, Jul. 2002.

[13] B. R. Cuenya, "Synthesis and catalytic properties of metal nanoparticles: Size, shape, support, composition, and oxidation state effects," Thin Solid Films, vol. 518, no. 12, pp. 3127–3150, Apr. 2010.

[14] Y. Khan et al., "Classification, synthetic, and Characterization Approaches to nanoparticles, and their applications in various fields of nanotechnology: a review," Catalysts, vol. 12, no. 11, p. 1386, Nov. 2022.].

[15] C. Iriarte-Mesa, Y. C. López, Y. Matos-Peralta, K. De La Vega-Hernández, and M. Antuch, "Gold, silver and iron oxide nanoparticles: Synthesis and bio-nanoconjugation strategies aiming to electrochemical applications," in Topics in current chemistry collections, 2020.

[16] Z. Alhalili, "Metal Oxides Nanoparticles: General Structural Description, Chemical, Physical, and Biological Synthesis Methods, Role in Pesticides and Heavy Metal Removal through Wastewater Treatment," Molecules/Molecules Online/Molecules Annual, vol. 28, no. 7, p. 3086, Mar. 2023.

[17] A. Aqel, K. M. M. A. El-Nour, R. A. Ammar, and A. Al-Warthan, "Carbon nanotubes, science and technology part (I) structure, synthesis and characterisation," Arabian Journal of Chemistry, vol. 5, no. 1, pp. 1–23, Jan. 2012.

[18] B. García-Pinel et al., "Lipid-Based Nanoparticles: Application and recent advances in cancer treatment," Nanomaterials, vol. 9, no. 4, p. 638, Apr. 2019.

[19] I. Venditti, "Morphologies and functionalities of polymeric nanocarriers as chemical tools for drug delivery: A review," Journal of King Saud University. Science, vol. 31, no. 3, pp. 398–411, Jul. 2019.

[20] D. Ma, "Hybrid nanoparticles," in Elsevier eBooks, 2019.

[21] S. Soares, J. Sousa, and A. Pais, "Nanomedicine: principles, properties, and regulatory issues," Frontiers in Chemistry, vol. 6, Aug. 2018.

[22] D. Sawah, M. Sahloul, and F. Ciftci, "Nano-material utilization in stem cells for regenerative medicine," Biomedizinische Technik, vol. 67, no. 6, pp. 429–442, Sep. 2022.

[23] S. Gavas, S. Quazi, and T. M. Karpiński, "Nanoparticles for cancer therapy: current progress and challenges," Nanoscale Research Letters, vol. 16, no. 1, Dec. 2021.

[24] Y. Omidi and J. Barar, "Targeting tumor microenvironment: crossing tumor interstitial fluid by multifunctional nanomedicines.," DOAJ (DOAJ: Directory of Open Access Journals), Jan. 2014.

[25] Q. Yang, S. W. Jones, C. L. Parker, W. C. Zamboni, J. E. Bear, and S. K. Lai, "Evading immune cell uptake and clearance requires PEG grafting at densities substantially exceeding the minimum for brush conformation," Molecular Pharmaceutics, vol. 11, no. 4, pp. 1250–1258, Mar. 2014.

[26] A. M. E. Shafey, "Green synthesis of metal and metal oxide nanoparticles from plant leaf extracts and their applications: A review," Green Processing and Synthesis, vol. 9, no. 1, pp. 304–339, Jun. 2020.

[27] T. Cele, 'Preparation of Nanoparticles', Engineered Nanomaterials - Health and Safety. IntechOpen, Jul. 08, 2020.

[28] H. Singh et al., "Revisiting the green synthesis of nanoparticles: uncovering influences of plant extracts as reducing agents for enhanced synthesis efficiency and its biomedical applications," International Journal of Nanomedicine, vol. Volume 18, pp. 4727–4750, Aug. 2023.

[29] Das SK, Dickinson C, Lafir F, Brougham DF, Marsili E. Synthesis, "Characterization and catalytic activity of gold nanoparticles biosynthesized with Rhizopus oryzae protein extract". Green Chem, 2012.

[30] Mondal A, Umekar MS, Bhusari GS, et al, "Biogenic Synthesis of Metal/Metal Oxide Nanostructured Materials." Curr Pharm Biotechnol, 2021.

[31] Rai M, Yadav A., "Plants as potential synthesizer of precious metal nanoparticles: progress and prospects." IET Nanobiotechnol, 2013.

[32] S. Bawazeer, "Green synthesis of silver nanoparticles from Euphorbia milii plant extract for enhanced antibacterial and enzyme inhibition effects," PubMed Central (PMC), Apr. 01, 2024.

[33] K. Saeed and I. Khan, "Preparation and characterization of single-walled carbon nanotube/nylon 6, 6 nanocomposites," Instrumentation Science & Technology, vol. 44, no. 4, pp. 435–444, Dec. 2015.

[34] J. Wang et al., "Accurate control of multishelled CO3O4 hollow microspheres as High-Performance anode materials in Lithium-Ion batteries," Angewandte Chemie, vol. 52, no. 25, pp. 6417–6420, May 2013.

[35] S. Mourdikoudis, R. M. Pallares, and N. T. K. Thanh, "Characterization techniques for nanoparticles: comparison and complementarity upon studying nanoparticle properties," Nanoscale, vol. 10, no. 27, pp. 12871–12934, Jan. 2018.

[36] Transmission electron microscopy and diffractometry of materials," SpringerLink.

[37] J. Tom PhD, "UV-VIS Spectroscopy: principle, strengths and limitations and applications," Analysis & Separations From Technology Networks, Dec. 18, 2023.].

[38] Peter. P. Fu, Q. Xia, H.-M. Hwang, P. C. Ray, and H. Yu, "Mechanisms of nanotoxicity: Generation of reactive oxygen species," Yàowù Shípǐn Fēnxī, vol. 22, no. 1, pp. 64–75, Mar. 2014.

[39] E. Girgis, W. K. B. Khalil, A. N. Emam, M. B. Mohamed, and K. V. Rao, "Nanotoxicity of gold and Gold–Cobalt nanoalloy," Chemical Research in Toxicology, vol. 25, no. 5, pp. 1086–1098, Apr. 2012

[40] Y.-H. Hsin, C.-F. Chen, S. Huang, T.-S. Shih, P.-S. Lai, and P. J. Chueh, "The apoptotic effect of nanosilver is mediated by a ROS- and JNK-dependent mechanism involving the mitochondrial pathway in NIH3T3 cells," Toxicology Letters, vol. 179, no. 3, pp. 130–139, Jul. 2008.

[41] Y. Wang, W. G. Aker, H.-M. Hwang, C. G. Yedjou, H. Yu, and P. B. Tchounwou, "A study of the mechanism of in vitro cytotoxicity of metal oxide nanoparticles using catfish primary hepatocytes and human HepG2 cells," Science of the Total Environment, vol. 409, no. 22, pp. 4753–4762, Oct. 2011

[42] A. V. Singh et al., "Review of emerging concepts in nanotoxicology: opportunities and challenges for safer nanomaterial design," Toxicol. Mech. Methods, vol. 29, no. 5, pp. 378–387, 2019.

[43] G. Oberdorster, "Safety assessment for nanotechnology and nanomedicine: concepts of nanotoxicology: Symposium: Nanotoxicological concepts," J. Intern. Med., vol. 267, no. 1, pp. 89–105, 2010.

[44] J. J. Giner-Casares, M. Henriksen-Lacey, M. Coronado-Puchau, and L. M. Liz-Marzán, "Inorganic nanoparticles for biomedicine: where materials scientists meet medical research," Mater. Today (Kidlington), vol. 19, no. 1, pp. 19–28, 2016.

[45] A. E. Nel et al., "Understanding biophysicochemical interactions at the nano–bio interface," Nat. Mater., vol. 8, no. 7, pp. 543–557, 2009.

[46] A. Sani, C. Cao, and D. Cui, "Toxicity of gold nanoparticles (AuNPs): A review," Biochem. Biophys. Rep., vol. 26, no. 100991, p. 100991, 2021.

[47] Y.-P. Jia, B.-Y. Ma, X.-W. Wei, and Z.-Y. Qian, "The in vitro and in vivo toxicity of gold nanoparticles," Chin. Chem. Lett., vol. 28, no. 4, pp. 691–702, 2017.

[48] Q. Xia, H. Li, Y. Liu, S. Zhang, Q. Feng, and K. Xiao, "The effect of particle size on the genotoxicity of gold nanoparticles: The effect of particle size on the genotoxicity of gold nanoparticles," J. Biomed. Mater. Res. A, vol. 105, no. 3, pp. 710–719, 2017.

[49] L. Yang, H. Kuang, W. Zhang, Z. P. Aguilar, H. Wei, and H. Xu, "Comparisons of the biodistribution and toxicological examinations after repeated intravenous administration of silver and gold nanoparticles in mice," Sci. Rep., vol. 7, no. 1, pp. 1–12, 2017.

[50] A. Rodriguez-Garraus, A. Azqueta, A. Vettorazzi, and A. López de Cerain, "Genotoxicity of silver nanoparticles," Nanomaterials (Basel), vol. 10, no. 2, p. 251, 2020.

[51] L. J. Hazeem et al., "Toxicity effect of silver nanoparticles on photosynthetic pigment content, growth, ROS production and ultrastructural changes of microalgae Chlorella vulgaris," Nanomaterials (Basel), vol. 9, no. 7, p. 914, 2019.

[52] Y. Zhang et al., "Silver nanoparticles decrease body weight and locomotor activity in adult male rats," Small, vol. 9, no. 9–10, pp. 1715–1720, 2013.

[53] W. H. De Jong et al., "Systemic and immunotoxicity of silver nanoparticles in an intravenous 28 days repeated dose toxicity study in rats," Biomaterials, vol. 34, no. 33, pp. 8333–8343, 2013.

[54] C.-K. Su, H.-T. Liu, S.-C. Hsia, and Y.-C. Sun, "Quantitatively profiling the dissolution and redistribution of silver nanoparticles in living rats using a

knotted reactor-based differentiation scheme," Anal. Chem., vol. 86, no. 16, pp. 8267–8274, 2014.

[55] Y. Xue et al., "Acute toxic effects and gender-related biokinetics of silver nanoparticles following an intravenous injection in mice: Acute toxic effects and gender-related biokinetics of AgNPs in mice," J. Appl. Toxicol., vol. 32, no. 11, pp. 890–899, 2012.

[56] H. Bahadar, F. Maqbool, K. Niaz, and M. Abdollahi, "Toxicity of nanoparticles and an overview of current experimental models.," PubMed, vol. 20, no. 1, pp. 1–11, Jan. 2016.

[57] N. Sharma et al., "Nanoparticles toxicity: an overview of its mechanism and plausible mitigation strategies," Journal of Drug Targeting, pp. 1–13, Feb. 2024.

[58] X. Cheng, Q. Xie, and Y. Sun, "Advances in nanomaterial-based targeted drug delivery systems," Frontiers in Bioengineering and Biotechnology, vol. 11, Apr. 2023.

[59] S. A. A. Rizvi and A. M. Saleh, "Applications of nanoparticle systems in drug delivery technology," Saudi Pharmaceutical Journal, vol. 26, no. 1, pp. 64–70, Jan. 2018.

[60] A. P. Singh, A. Biswas, A. Shukla, and P. Maiti, "Targeted therapy in chronic diseases using nanomaterial-based drug delivery vehicles," Signal Transduction and Targeted Therapy, vol. 4, no. 1, Aug. 2019,

[61] C. C. González, A. L. Piñón-Urbina, and P. E. García-Casillas, "Synthesis of Controlled-Size Silica Nanoparticles from Sodium Metasilicate and the Effect of the Addition of PEG in the Size Distribution," Materials, vol. 11, no. 4, p. 510, Mar. 2018.

[62] M. Shaban and M. Hasanzadeh, "Biomedical applications of dendritic fibrous nanosilica (DFNS): recent progress and challenges," RSC Advances, vol. 10, no. 61, pp. 37116–37133, Jan. 2020

[63] B. V. Salas and A. A. S. Navarro, "Synthesis of silica nanoparticles from sodium metasilica tmilii," International Journal of Nanoparticles (Print), vol. 14, no. 1, p. 1, Jan. 2022.

[64] S. Prabha, D. Durgalakshmi, S. Rajendran, and E. Lichtfouse, "Plant-derived silica nanoparticles and composites for biosensors, bioimaging, drug delivery and supercapacitors: a review," Environmental Chemistry Letters, vol. 19, no. 2, pp. 1667–1691, Nov. 2020

[65] V. Selvarajan, S. A. O. Obuobi, and P. L. R. Ee, "Silica Nanoparticles—A versatile tool for the treatment of bacterial infections," Frontiers in Chemistry, vol. 8, Jul. 2020.

[66] D. A. S. Razo et al., "A version of Stöber synthesis enabling the facile prediction of silica nanospheres size for the fabrication of opal photonic crystals," Journal of Nanoparticle Research, vol. 10, no. 7, pp. 225–1229, 2008.

[67] M. A. Sharaf and I. A. M. Ibrahim, "Preparation of spherical nanoparticles: Stober silica," ResearchGate, 2010.

[68] Q. Guo et al., "Synthesis of disperse amorphous SiO2 nanoparticles via sol–gel process," Ceramics International, vol. 43, no. 1, pp. 192–196, 2017.

[69] H. N. Azlina, J. N. Hasnidawani, H. Norita, and S. N. Surip, "Synthesis of SIO2Nanostructures using Sol-Gel method," Acta Physica Polonica. A, vol. 129, no. 4, pp. 842–844, 2016.

[70] A. A. W. Hajarul, D. Z. Nor, A. A. Aziz, and A. R. Khairunisak, "Properties of amorphous silica entrapped isoniazid drug delivery system," Advanced Materials Research, vol. 364, pp. 134–138, 2011.

[71] M. a. A. Badr, A. A. I. Khalil, M. M. H. Khalil, A. Hafez, and E. M. Mostafa, "Green Synthesis of Silica- Polysaccharides Nano- composites from Sodium Silicate and Aloe Vera gel for Self-cleaning of Solar Mirrors," Research Square (Research Square), Jan. 2024.

[72] M. Kumari, K. Singh, P. Dhull, R. K. Lohchab, and A. K. Haritash, "Sustainable Green approach of silica nanoparticle synthesis using an agro-waste rice

husk," Nature, Environment and Pollution Technology/Nature, Environment and Pollution Technology, vol. 22, no. 1, pp. 477–487, Mar. 2023.

[73] S. Azizi, J. Soleymani, and N. Shadjou, "Synthesis of folic acid functionalized terbium-doped dendritic fibrous nano-silica and Interaction withHEK293 normal,MDAbreast cancer andHT29 colon cancer cells," JMR. Journal of Molecular Recognition/Journal of Molecular Recognition, vol. 33, no. 11, Jul. 2020.

[74] A. V. V. Nikezić, A. M. Bondžić, and V. M. Vasić, "Drug delivery systems based on nanoparticles and related nanostructures," European Journal of Pharmaceutical Sciences, vol. 151, p. 105412, Aug. 2020.

[75] N. U. Khaliq et al., "Mesoporous silica nanoparticles as a gene delivery platform for cancer therapy," Pharmaceutics, vol. 15, no. 5, p. 1432, May 2023.

[76] A. Watermann and J. Brieger, "Mesoporous silica nanoparticles as drug delivery vehicles in cancer," Nanomaterials, vol. 7, no. 7, p. 189, Jul. 2017.

[77] U. Zulfiqar, T. Subhani, and S. W. Husain, "Synthesis of silica nanoparticles from sodium silicate under alkaline conditions," Journal of Sol-gel Science and Technology, vol. 77, no. 3, pp. 753–758, Jan. 2016.

[78] H. Kaur, S. Chaudhary, H. Kaur, M. Chaudhary, and K. C. Jena, "Hydrolysis and condensation of tetraethyl orthosilicate at the Air–Aqueous interface: Implications for silica nanoparticle formation," ACS Applied Nano Materials, vol. 5, no. 1, pp. 411–422, Dec. 2021.

[79] C. Chapa-González, A. Piñón-Urbina, and P. García-Casillas, "Synthesis of Controlled-Size Silica Nanoparticles from Sodium Metasilicate and the Effect of the Addition of PEG in the Size Distribution," Materials, vol. 11, no. 4, p. 510, Mar. 2018.

[80] H. Saleem et al., "In vitro biological propensities and chemical profiling of Euphorbia milii Des Moul (Euphorbiaceae): A novel source for bioactive agents," Industrial Crops and Products, vol. 130, pp. 9–15, Apr. 2019.

[81] M. Inoue, S. Hayashi, and L. E. Craker, "Role of Medicinal and Aromatic plants: past, present, and future," in IntechOpen eBooks, 2019.

[82] Shobana F and Vinusha C: "Phytochemical screening and antimicrobial studies in leaf extract." International Journal for Multidisciplinary Research, 2015.

[83] PlantPals, "What is a crown of thorns plant? - PlantPals - Medium," Medium, Aug. 22, 2023.

[84] Y. He et al., "Diverse diterpenoids with $\alpha$-glucosidase and $\beta$-glucuronidase inhibitory activities from Euphorbia milii," Phytochemistry, vol. 196, p. 113106, Apr. 2022.

[85] Rauf A, Naveed M, Muhammad Q, Ghias U and Iftikhar H., " Preliminary Antinociceptive Studies of Methanol Extract of Euphorbia milii," Middle-East Journal of Medicinal Plants Research, 2012.

[86] Ks. Dipen, Kt. Divya, Ps. Kirtan, Ps. Ashish, and Ks. Avinash, "Extract of Euphorbia milii flower: A natural indicator in acid-base titration," Journal of Integrated Health Sciences, vol. 4, no. 2, p. 2, Jan. 2016.

[87] R. L. Besagas and M. C. D. Gapuz, "Phytochemical profiles and antioxidant activities of leaf extracts of euphorbia species," ResearchGate, Jan. 2018.

[88] Yadav S.C, Pande M and Jagannadham MV, "Highly stable glycosylated serine protease from the medicinal plant Euphorbia milii." Phytochemistry, 2006.

[89] F. Zeghad, S. E. Djılanı, A. Djılanı, and A. Dıcko, "Antimicrobial and antioxidant activities of three Euphorbia species," Turkish Journal of Pharmaceutical Sciences, vol. 13, no. 1, pp. 22–37, Jan. 2016.

[90] W. A. Negm et al., "Phytochemical inspection and anti-inflammatory potential of Euphorbia milii Des Moul. integrated with network pharmacology approach," Arabian Journal of Chemistry, vol. 17, no. 2, p. 105568, Feb. 2024.

[91] H. Zhao et al., "Phytochemical and pharmacological review of diterpenoids from the genus Euphorbia Linn (2012–2021)," Journal of Ethnopharmacology, vol. 298, p. 115574, Nov. 2022.

[92] S. Bawazeer, "Green synthesis of silver nanoparticles from Euphorbia milii plant extract for enhanced antibacterial and enzyme inhibition effects," PubMed Central (PMC), Apr. 01, 2024.

[93] S. Venkatesan et al., "Biosynthesis of zinc oxide nanoparticles using Euphorbia milii leaf constituents: Characterization and improved photocatalytic degradation of methylene blue dye under natural sunlight," Journal of the Indian Chemical Society, vol. 99, no. 5, p. 100436, May 2022.

[94] S. Patil, "Phytochemical Study and Antioxidant Properties of Ethanolic Extracts of Euphorbia milii.," Feb. 10, 2020.

[95] C. Y. Rahimzadeh, A. A. Barzinjy, A. S. Mohammed, and S. M. Hamad, "Green synthesis of SiO2 nanoparticles from Rhus coriaria L. extract: Comparison with chemically synthesized SiO2 nanoparticles," PloS One, vol. 17, no. 8, p. e0268184, Aug. 2022

[96] R. A. Pratiwi and A. B. D. Nandiyanto, "How to read and interpret UV-VIS spectrophotometric results in determining the structure of chemical compounds," Indonesian Journal of Educational Research and Technology, vol. 2, no. 1, pp. 1-20, 2022.

[97] A. Mazzaglia et al., "Supramolecular Colloidal Systems of Gold Nanoparticles/Amphiphilic Cyclodextrin: a FE-SEM and XPS Investigation of Nanostructures Assembled onto Solid Surface," Journal of Physical Chemistry. C./Journal of Physical Chemistry. C, vol. 113, no. 29, pp. 12772–12777, Jun. 2009.

[98] J. S. Gaffney, N. A. Marley, and D. E. Jones, "Fourier Transform Infrared ( FTIR ) Spectroscopy," Characterization of Materials, pp. 1–33, Oct. 2012.

[99] B. K. Mehta, M. Chhajlani, and B. D. Shrivastava, "Green synthesis of silver nanoparticles and their characterization by XRD," Journal of Physics: Conference Series, vol. 836, p. 012050, 2017.

[100] S. Bhoye, A. Somkuwar, K. Sarode, S. Dubey, and H. Harke, "Effect of Aloe vera gel and mint tea on letrozole induced PCOS in rat model," Journal of Pharmacognosy and Phytochemistry, vol. 10, no. 3, pp. 494–499, 2021.

[101] R. Gobinath, S. Parasuraman, S. Sreeramanan, B. Enugutti, and S. V. Chinni, "Antidiabetic and Antihyperlipidemic Effects of Methanolic Extract of Leaves of Spondias mombin in Streptozotocin-Induced Diabetic Rats," Frontiers in Physiology, vol. 13, May 2022.

[102] V. Gmoshinski et al., "Toxicity Evaluation of nanostructured silica orally administered to rats: influence on immune system function," Nanomaterials, vol. 10, no. 11, p. 2126, Oct. 2020.

[103] S. Mukherjee et al., "Acute toxicity, biodistribution, and pharmacokinetics studies of pegylated platinum nanoparticles in mouse model," Adv. Nanobiomed Res., vol. 1, no. 7, p. 2000082, 2021.

[104] Pandey, P. Dabhade, and A. Kumarasamy, "Inflammatory effects of subacute exposure of Roundup in rat liver and adipose tissue," Dose Response, vol. 17, no. 2, p. 1559325819843380, 2019.

[105] F. Masjedi, A. Gol, and S. Dabiri, "Preventive effect of garlic (Allium sativum L.) on serum biochemical factors and histopathology of pancreas and liver in Streptozotocin- induced diabetic rats," Iranian Journal of Pharmaceutical Research, vol. 12, no. 3, pp. 325–338, 2013.

[106] H. A. Khan et al., "Green synthesis of silver nanoparticles from plant Fagonia cretica and evaluating its anti-diabetic activity through in-depth in-vitro and in-vivo analysis," Frontiers in Pharmacology, vol. 14, Oct. 2023.

[107] Jasco, "Principles of infrared spectroscopy (4) Advantages of FTIR spectroscopy | JASCO Global," JASCO Inc., Sep. 16, 2022.

[108] R. Padhye, A. J. A. Aquino, D. Tunega, and M. L. Pantoya, "Effect of polar environments on the aluminum oxide shell surrounding aluminum particles: simulations of surface hydroxyl bonding and charge," ACS Applied Materials & Interfaces, vol. 8, no. 22, pp. 13926–13933, May 2016.

[109] M. H. S. Abadi, A. Delbari, Z. Fakoor, and J. Baedi, "Effects of annealing temperature on infrared spectra of SIO2 extracted from rice husk," ResearchGate, Dec. 2014.

[110] P. Sharma, J. Kherb, J. Prakash, and R. Kaushal, "A novel and facile green synthesis of SiO2 nanoparticles for removal of toxic water pollutants," Applied Nanoscience, vol. 13, no. 1, pp. 735–747, Jun. 2021.

[111] D. C. Lingegowda, K.. K. J, S. Gopal, Deviparsad, and M. Zarei, "FTIR spectroscopic studies on cleome gynandra – comparative analysis of functional group before and after extraction," ResearchGate, 2013.

[112] K. S. Rani, M. Mumtaz, R. Priyank, and M. Chandran, "Phytochemical screening by FTIR spectroscopic analysis of methanol leaf extract of herb Andrographis echioides," Journal of Ayurvedic and Herbal Medicine, vol. 7, no. 4, pp. 257–261, 2021.

[113] K.-M. Li, J.-G. Jiang, S.-C. Tian, X.-J. Chen, and F. Yan, "Influence of silica types on synthesis and performance of Amine–Silica hybrid materials used for CO2 capture," Journal of Physical Chemistry. C./Journal of Physical Chemistry. C, vol. 118, no. 5, pp. 2454–2462, Jan. 2014.

[114] C. Yuen, S. Ku, P. Choi, C. Kan, and S. Tsang, "Determining functional groups of commercially available Ink-Jet printing reactive dyes using infrared spectroscopy," 2005.

[115] A. Suryavanshi, S. Kumar, and D. K. Arya, "Evaluation of phytochemical and antibacterial potential of Ajuga parviflora Benth.," Medicinal Plants, vol. 12, no. 1, p. 144, Jan. 2020.

[116] A. I. Biradar, P. D. Sarvalkar, S. B. Teli, C. A. Pawar, P. S. Patil, and N. R. Prasad, "Photocatalytic degradation of dyes using one-step synthesized silica nanoparticles," Materials Today: Proceedings, vol. 43, pp. 2832–2838, Jan. 2021.

[117] M. Hatami, M. Ahmadipour, and S. Asghari, "Heterocyclic grafting functionalization of silica nanoparticles: fabrication, morphological investigation and application for PVA nanocomposites," Journal of Inorganic and Organometallic Polymers and Materials, vol. 27, no. 4, pp. 1072–1083, Apr. 2017.

[118] T. Hao et al., "Emerging applications of silica nanoparticles as multifunctional modifiers for high performance polyester composites," Nanomaterials, vol. 11, no. 11, p. 2810, Oct. 2021.

[119] R. Manikandan and J. Thomas, "Sustainable approaches in green synthesis of silica nanoparticles using extracts of chlorella and its application," Applied Biochemistry and Biotechnology, Apr. 2024.

[120] Azeez. A. Barzinjy, S. M. Hamad, and H. J. Ismael, "Characterization of ZnO Nanoparticles Prepared from Green Synthesis Using Euphorbia Petiolata Leaves," Eurasian Journal of Science and Engineering, vol. 4, no. 3, Jan. 2019.

[121] M. Sultana, S. Tabassum, S. M. Ullah, and M. S. Bashar, "Structural, optical, and morphological characterization of silica nanoparticles prepared by Sol-Gel Process," Journal of the Turkish Chemical Society, Section A: Chemistry, vol. 9, no. 4, pp. 1323–1334, Nov. 2022.

[122] N. N. Aien Mohamed AbdulGhani, M. A. Saeed, and I. H. Hashim, "Thermoluminescence (TL) response of silica nanoparticles subjected to 50 Gy gamma irradiation.," Malaysian Journal of Fundamental and Applied Sciences, vol. 13, no. 3, 2017.

[123] H.-Y. Han, "Sublethal pulmonary toxicity screening of silica nanoparticles in rats after direct intratracheal instillation," Toxicological Research, vol. 38, no. 4, pp. 523–530, May 2022.

[124] Sreenika. G, Naga Sravanthi. K, Lakshmi. BVS, Thulja. P, and Sudhakar. M., "Antioxidant and antitumor activity of euphorbia milii flower extract against in vivo breast cancer and colon cancer in mice.," world journal of pharmacy and pharmaceutical sciences, vol. 4, no. 06, 912–934, 2015.

[125] T. N. Almanaa et al., "Silica Nanoparticle Acute Toxicity on Male Rattus norvegicus Domestica: Ethological Behavior, Hematological Disorders, Biochemical Analyses, Hepato-Renal Function, and Antioxidant-Immune Response," Frontiers in Bioengineering and Biotechnology, vol. 10, Apr. 2022.

[126] Z. Du et al., "Silica nanoparticles induce cardiomyocyte apoptosis via the mitochondrial pathway in rats following intratracheal instillation," International Journal of Molecular Medicine, Dec. 2018.

[127] C. O. Okonkwo, O. C. Ohaeri, and I. J. Atangwho, "Haematological changes in rats exposed to insecticidal oils from the leaves of Cassia occidentalis and Euphorbia milii," Heliyon, vol. 5, no. 5, p. e01746, May 2019.

[128] Z. Zhang et al., "Relationship between Red Blood Cell Indices (MCV, MCH, and MCHC) and Major Adverse Cardiovascular Events in Anemic and Nonanemic Patients with Acute Coronary Syndrome," Disease Markers, vol. 2022, pp. 1–12, Nov. 2022.

[129] C. L. Liang et al., "Subchronic oral toxicity of silica nanoparticles and silica microparticles in rats.," PubMed, vol. 31, no. 3, pp. 197–207, Mar. 2018.

[130] A. Ismail, N. Sial, R. Rehman, S. Abid, and M. S. Ismail, "Survival, growth, behavior, hematology and serum biochemistry of mice under different concentrations of orally administered amorphous silica nanoparticle," Toxicology Reports, vol. 10, pp. 659–668, Jan. 2023.

[131] Liver function tests: indication and interpretation - The Pharmaceutical Journal," The Pharmaceutical Journal, Aug. 15, 2022. https://pharmaceutical-journal.com/article/ld/liver-function-tests-indication-and-interpretation.

[132] J. Van De Wouw and J. A. Joles, "Albumin is an interface between blood plasma and cell membrane, and not just a sponge," Clinical Kidney Journal, vol. 15, no. 4, pp. 624–634, Oct. 2021.

[133] J. F. De Brito Galvao and S. A. Center, "Fluid, electrolyte, and Acid-Base disturbances in liver disease," in Elsevier eBooks, 2012, pp. 456–499.

[134] M. L. Bishop, E. P. Fody, and L. E Schoeff, Clinical Chemistry: principles, techniques and correlations PDF Download, 7th ed. 2024.

[135] S. Yadav, R. Jangra, B. R. Sharma, and M. Sharma, "Current Advancement in Biosensing techniques for determination of Alanine aminotransferase and Aspartate aminotransferase-a Mini Review," Process Biochemistry, vol. 114, pp. 71–76, Mar. 2022.

[136] W.-T. Chan et al., "In vivo toxicologic study of larger silica nanoparticles in mice," International Journal of Nanomedicine, vol. Volume 12, pp. 3421–3432, Apr. 2017.

[137] A. Ali et al., "Synthesis and characterization of silica, Silver-Silica, and zinc Oxide-Silica nanoparticles for evaluation of blood biochemistry, oxidative stress, and hepatotoxicity in albino rats," ACS Omega, vol. 8, no. 23, pp. 20900–20911, Jun. 2023.

[138] D. Arifianto, D. Adji, B. Sutrisno, and N. Rickyawan, "Renal histopathology, blood urea nitrogen and creatinine levels of rats with unilateral ureteral obstruction," ResearchGate, Jul. 2020.

[139] A. M. Mahmoud et al., "Mesoporous silica nanoparticles trigger liver and kidney injury fibrosis via altering TLR4/NF-KB, JAK2/STAT3 and NRF2/HO-1 signaling in rats," Biomolecules, vol. 9, no. 10, p. 528, Sep. 2019.

[140] R. Rehman, S. Khanam, Y. Khan, and F. Hayat, "Toxicological effects of colloidal silver nanoparticles on rat health: Assessing physiological, hematological, biochemical, and behavioral parameters," Deleted Journal, vol. 2, no. 1, pp. 101–107, Jun. 2024.

[141] N. R. Sproston and J. J. Ashworth, "Role of C-Reactive protein at sites of inflammation and infection," Frontiers in Immunology, vol. 9, Apr. 2018.

[142] V. Castranova, L. Millecchia, J. Y. C. Ma, A. F. Hubbs, and A. Teass, "Effect of inhaled crystalline silica in a rat model: time course of pulmonary reactions," PubMed, Jun. 01, 2002.

[143] A. Passos et al., "Red blood cell sedimentation rate measurements in a high aspect ratio microchannel," Clinical Hemorheology and Microcirculation, vol. 82, no. 4, pp. 313–322, Dec. 2022.

[144] M. Silitonga and P. M. Silitonga, "Haematological profile of rats (Rattus norvegicus) induced BCG and provided leaf extract of Plectranthus amboinicus Lour Spreng)," AIP Conference Proceedings, Jan. 2017.

[145] A. Abulikemu et al., "Silica nanoparticles aggravated the metabolic associated fatty liver disease through disturbed amino acid and lipid metabolisms-mediated oxidative stress," Redox Biology, vol. 59, p. 102569, Feb. 2023.

[146] M. R. Shahein et al., "Impact of Incorporating the Aqueous Extract of Hawthorn (C. oxyanatha) Leaves on Yogurt Properties and Its Therapeutic Effects against Oxidative Stress Induced by Carbon Tetrachloride in Rats," Fermentation, vol. 8, no. 5, p. 200, Apr. 2022.